TITLE:

Purified Zymogens Reveal Mechanisms of Snake Venom Metalloproteinase Auto-Activation

AUTHORS:

Sophie Hall[1], Iara Aimê Cardoso[1], Mark C. Wilkinson[2], Maria Molina Carretero[3], Srikanth Lingappa[1], Bronwyn Rand[1], Dakang Shen[1], Johara Boldrini-França[1], Richard Stenner[1], Stefanie K. Menzies[2,4], Georgia Balchin[1], Konrad Kamil Hus[1,5], Renaud Vincentelli[6], Andrew Mumford[3], Nicholas R. Casewell[2], Imre Berger[1,7]*, Christiane Schaffitzel[1]*

AFFILIATIONS:

[1] School of Biochemistry, University of Bristol, University Walk, Bristol BS8 1TD, UK

[2] Centre for Snakebite Research and Interventions, Liverpool School of Tropical Medicine, Liverpool L3 5QA, UK

[3] School of Cellular and Molecular Medicine, University of Bristol, 1 Tankard's Close, Bristol BS8 1TD, UK

[4] Lancaster University, Bailrigg, Lancaster, United Kingdom

[5] Department of Biotechnology and Bioinformatics, Faculty of Chemistry, Rzeszow University of Technology, Powstancow Warszawy 6, 35-959 Rzeszow, Poland

[6] Architecture et Fonction des Macromolécules Biologiques (AFMB), UMR 7257 CNRS-Aix-Marseille Université, 13288 Marseille, France

[7] Max Planck Bristol Centre for Minimal Biology, School of Chemistry, University of Bristol, Cantock's Close, Bristol BS8 1TS, UK

For Correspondence:

Christiane Schaffitzel, email: christiane.berger-schaffitzel@bristol.ac.uk

Imre Berger, email: imre.berger@bristol.ac.uk

ABSTRACT

Snake venoms contain diverse mixtures of toxins that evolved to incapacitate prey, but in humans they cause extensive pathology following snakebite envenomation. In viper venom, the most potent toxins are the haemorrhagic and coagulopathic snake venom metalloproteinases (SVMPs). Because venoms contain a SVMP cocktail, and due to their cytotoxicity, SVMP characterizations have been hampered by the lack of purified enzymes. By incorporating their prodomain, which blocks the active SVMP site, we overcame their cytotoxicity and enabled recombinant production of zymogens from all three structurally variable SVMP classes (PI, PII and PIII) using our baculovirus/insect cell expression system. Zymogens were auto-activated by incubation with Zn^{2+} ions, resulting in prodomain cleavage, PII disintegrin cleavage and PIII prodomain proteolysis. Auto-activated SVMPs were characterized using protein substrate degradation, platelet aggregation and blood coagulation assays, benchmarked to native venom-purified SVMP. Our recombinant zymogen production protocol is generically applicable for the expression of SVMPs, unlocking biomedical use in haematology, and discovery of novel snakebite therapeutics.

INTRODUCTION

Snake venom is a complex cocktail of more than 100 proteins and peptides belonging to various toxin families (*1*). Although the number and abundance of isoforms within these families vary extensively across different venomous snakes, the snake venom metalloproteinases (SVMP) are a pathologically important toxin family present in almost all snake venoms. SVMPs play a significant role in the physiological effects resulting from both local and systemic envenoming, such as haemorrhage, coagulopathy and tissue necrosis (*2*). In many medically important viperid snake genera such as *Echis* (saw-scaled vipers), SVMP toxins are the most abundant toxin constituents, on average accounting for 33% of all toxins, though this can be as high as 72% in *Echis ocellatus* (*3-5*) (Fig. 1a).

SVMPs are complex, structurally variable, cysteine-rich, Zn^{2+}-dependent metalloproteinases that can be classified into three sub-classes based on domain architecture: PI (comprising metalloproteinase domain only), PII (metalloproteinase and disintegrin domains) and PIII (metalloproteinase, disintegrin-like and cysteine-rich domains) (Fig. 1b); representatives of all three sub-classes are present in viper venom.

SVMPs are particularly toxic proteins with a wide range of substrates. They are known to degrade the basement membrane and extracellular matrix proteins, as well as several blood clotting factors, most notably fibrinogen, through their metalloproteinase domain (*6, 7*). Extracellular matrix breakdown and loss in blood capillary wall integrity results in vascular leakage, resulting in both local and systemic haemorrhage (*8*) and in the spread of other venom toxins (*9*). In PII SVMPs, the disintegrin domain contains a charged, integrin-binding motif, most commonly an arginine-glycine-aspartate (RGD) motif, which binds, among others, the fibrinogen receptor integrin $\alpha_{IIb}\beta_3$ (*10*), causing inhibition of platelet aggregation.

Because viper SVMPs often target components of the coagulation cascade with unique specificity and/or lack of reliance on typically essential co-factors, these enzymes are highly valuable for investigating and monitoring the treatment of pathologies related to haemostasis (e.g. factor deficiencies, bleeding disorders) (*11*). In the clinic, the SVMPs RVV-X and Ecarin are both used as standards for coagulation tests (*12*). In addition, SVMP-derived disintegrins have been repurposed for use as, or inspiration for the design of, anti-platelet therapies to treat atherothrombosis in the form of unstable angina and myocardial infarction (*1*). Thus, a single snake venom toxin family has yielded several translationally valuable tools for diagnosis and treatment of human disease. However, further exploitation of SVMPs is hampered by the considerable challenge in purifying individual SVMP proteins from venom, and the lack of robust, scalable, recombinant toxin production protocols, representing a bottleneck.

51 Currently, SVMPs are typically purified from venom by size exclusion chromatography (SEC),
52 followed by ion exchange chromatography of the peaks containing SVMPs. Further separation
53 can be achieved by hydrophobic interaction chromatography or reversed-phase high
54 performance liquid chromatography (RP-HPLC) (*13, 14*). However, complete separation of
55 endogenous functionally active SVMPs is difficult to achieve, because: (i) many venoms
56 contain multiple related SVMP isoforms that share similar physicochemical properties, (ii) the
57 resulting yields of each particular SVMP isoform can be very low, and (iii) the use of some
58 desirable separation approaches (e.g. RP-HPLC) can result in SVMP denaturation.
59 Importantly, this procedure is impeded by the limited access to sufficient amounts of extracted
60 snake venom.

61 Recombinant expression of SVMPs could resolve the bottleneck, but is severely hampered by
62 their cytotoxicity, domain complexity and high number of cysteine residues that complicate
63 protein folding - for example, the PIII SVMPs contain between 20 and 40 cysteines forming
64 disulfides (*15*). Currently, protocols are available for the production of only a select few specific
65 SVMPs (including albocollagenase, bothropasin and Ecarin) (*16-18*). However, these suffer
66 from limitations such as low yield and inactive proteins. Zymogen production of SVMPs has
67 been described before, but it remains generally elusive how the zymogen is processed into
68 the mature, active SVMP. Current protocols describe incubation of the zymogen for >7 days
69 (*18*), incubation with other active proteinase toxins (*19*), or the insertion of a TEV protease
70 cleavage site into the SVMP amino acid sequence (*20*).

71 Here, we establish a novel and generic protocol to access functional PI, PII and PIII SVMPs
72 in the quality and quantity required for characterizations and show that all three classes of
73 SVMPs can auto-activate in the presence of zinc ions, resulting in distinct outcomes.

74 We used our MultiBac baculovirus/insect cell expression system (*21*) for recombinant SVMP
75 zymogen production. The MultiBac system is well-established for secretion of proteins,
76 including the C-terminal heavy chain domain of the highly toxic protein, clostridial botulinum
77 neurotoxin (*22*). We postulate that this system is highly suitable for SVMP production because
78 (i) folding of the multi-domain SVMP zymogen will be supported by eukaryotic, endogenous
79 chaperones present in insect cells and (ii) secreted SVMPs will undergo cellular protein quality
80 control in the endoplasmic reticulum (ER) and Golgi apparatus for correct disulfide bond
81 formation and glycosylation before secretion, ensuring that the toxins produced are correctly
82 folded, soluble and authentically modified. We show that zymogen expression overcomes
83 SVMP cytotoxicity, and we demonstrate successful production of PI and PII SVMPs from *Echis*
84 *ocellatus* and a PIII SVMP from *Echis carinatus sochureki* (Fig. 1b,c). We establish auto-
85 activation of the SVMP zymogens and concomitant cleavage of the prodomain (all classes),
86 C-terminal tags (PI, PII) and the disintegrin domain (PII). The PIII prodomain is completely

87 degraded by the activated SVMP. We further analyse the cytotoxicity and haemotoxicity of the
88 auto-activated SVMPs *in vitro* using established casein (*23*), fibrinogen (*23*), fluorogenic
89 peptide (*24*) and insulin degradation (*13*) assays. For the PI SVMP, we show that the substrate
90 specificity of recombinant SVMP is identical to that of the corresponding toxin purified from
91 venom, compellingly validating the utility of our strategy.

92 Our generic SVMP production protocol thus paves the way to systematically characterize
93 SVMPs and unlock biomedical applications, in haematology, thrombosis and inflammation
94 research and as targets for the discovery of novel snakebite therapeutics.

95 **RESULTS**

96 **Recombinant SVMP zymogen expression overcomes their cytotoxicity.**

97 For our expression trials, we chose PI, PII and PIII SVMPs which, according to transcriptomics
98 (*25*), are highly expressed in the venom gland of medically important vipers in Sub-Saharan
99 Africa. We generated baculovirus/insect cell expression constructs for Q2UXQ3 (PI),
100 A0A3G1E3U2 (PII) and E9JG34 (PIII) (Fig. 1c), each encoding a melittin signal sequence for
101 secretion, the toxin of interest and C-terminal tandem hexahistidine- and Avi-tags (*26*), codon
102 optimized for both *Spotoptera frugiperda* and *Trichoplusia Ni* as expression hosts. Initially,
103 recombinant production of mature SVMPs, without the N-terminally fused prodomain, was
104 attempted (Fig. 2a-c). Protein expression yields, however, were extremely low, primarily due
105 to SVMP cytotoxicity causing cell death immediately upon baculoviral infection. This was
106 evidenced by very low cell viability, with more than 60% of cells dying within 72 hours of
107 expression, and 100% cell death by 96 hours into the expression for the PI and PIII SVMPs
108 (Fig. 2a). Yellow fluorescent protein (YFP) is used in the MultiBac expression system as an
109 indicator of baculovirus performance and a proxy for heterologous protein production (*21*).
110 Typically, YFP fluorescence is followed during expression and cells/proteins are harvested
111 when YFP production reaches a plateau (*21*). Throughout mature SVMP expression, YFP
112 fluorescence remained very low, consistent with pervasive premature cell death caused by the
113 SVMP toxin resulting in low YFP production, and cell lysis leading to release of YFP into the
114 media (Fig. 2b). Additionally, the decrease in YFP readings observed (days 3-5 after
115 proliferation arrest) during expression could also be due to proteolytic degradation of YFP by
116 the mature, active SVMP.

117 Western blot analysis detecting the His-tag fused C-terminally to the SVMP, showed that the
118 mature PI and PIII had been successfully expressed within the cells. It also indicated that
119 these SVMPs were soluble because they could be detected not only in the whole cell extract
120 (SNP; combined supernatant/pellet) but also in the cleared lysate (SN; supernatant) (Fig. 2c).
121 However, no SVMP was detected in the media sample in the Western blot, indicating that little
122 or no SVMP had been secreted. This is possibly due to the premature death and lysis of the
123 cells, caused by the toxin, impairing the secretion machinery before noticeable secretion had
124 occurred. Taken together, expression of mature SVMPs detrimentally affects cell integrity,
125 damaging the cells early after baculovirus infection and as soon as protein production initiates,
126 underscoring the toxicity of the SVMPs.

127 Therefore, subsequent expression strategies to produce SVMPs were aimed at inactivating
128 the metalloproteinase. We first tested Marimastat, a broad-spectrum metalloproteinase
129 inhibitor (*27*). Marimastat binds to the active site of the metalloproteinase mimicking the
130 structure of a peptide substrate, inhibiting SVMP activity (*27*). During baculovirus infection,

131 Marimastat was added to the medium at a final concentration of 3 μM and 6 μM, respectively
132 (Fig. S1a). At these concentrations however, Marimastat could not prevent cell death induced
133 by PIII SVMP expression. On the contrary, the cell viability in the presence of 3 μM and 6 μM
134 Marimastat was even further decreased. Additionally, less SVMP was detected in anti-His-tag
135 Western blots in whole cell extract (SNP) and cleared lysate (SN), compared to the expression
136 of mature SVMP without Marimastat (Fig. S1a). Thus, Marimastat itself appears to be toxic to
137 insect cells at the doses tested and has no positive effect on SVMP expression and recovery.

138 Next, we tested SVMP active site mutants based on a previous report of an inactive PII SVMP
139 purified from *Bothriechis lateralis* venom (*28*). Two active site mutations were identified in the
140 protein rendering it inactive (canonical sequence: HEXXHXXGXXH, inactive sequence:
141 H**D**LGHNL**C**IDH). We inserted these mutations into our PI and PIII SVMPs. We found
142 improved cell viability and detected elevated YFP signal for the PI SVMP active site mutant
143 (Fig. S1b). However, the PIII SVMP active site mutant still showed significant toxicity, reducing
144 YFP levels as well as cell viability. Nonetheless, we successfully purified both PI and PIII
145 SVMP active site mutants from the media using immobilized metal affinity purification (IMAC)
146 via the hexahistidine tags present in our proteins. Based on our observations with the active
147 site mutants, we concluded that inhibition of metalloproteinase activity during SVMP protein
148 production has a positive effect, indicating that expressing inactivated SVMPs could be a
149 viable, although inefficient, approach.

150 In the snake venom gland, SVMPs are produced with an N-terminally fused prodomain that is
151 removed through cleavage during post-translational processing of the protein (Fig. 2d). The
152 prodomain comprises a small, highly conserved propeptide sequence (usually PKMCGVT) -
153 this propeptide acts as a cysteine switch to maintain enzyme latency (*29*). AlphaFold 2 (*30*)
154 predicts that the prodomain adopts a β-barrel structure and folds around the metalloproteinase
155 (MP) domain, slotting the propeptide into the active site of the MP domain, where the
156 propeptide cysteine co-ordinates the active site Zn^{2+} ion, along with the three active site
157 histidines (Fig. 2d). This renders the MP inactive as the Zn^{2+} ion cannot be accessed by
158 substrates in the active site. Inspired by this, we designed propeptide-SVMP fusion proteins
159 using the propeptide responsible for the cysteine switch, PKMCGVT. We fused three
160 propeptide repeats to the N-terminus of the SVMP followed by a TEV protease cleavage site.
161 We hypothesized that this would increase the avidity of the propeptide to the MP active site
162 and efficiently inactivate the enzyme. Cell viability for the propeptide-SVMP fusion expression
163 trials was higher at days 3-5 when compared to the mature SVMPs (Fig. 2a and 2e). However,
164 towards the end of expression less than 25% of cells were left alive (day 5), likely limiting
165 protein secretion. Although YFP fluorescence levels for PI and PIII had slightly increased (Fig.
166 2f) compared to expression of the mature SVMP (Fig. 2b), YFP expression was still

167 significantly lower as compared to a positive control which expressed an unrelated, non-toxic
168 protein. Western blot analysis confirmed that PI and PIII SVMPs were expressed and soluble
169 (Fig. 2g). However, propeptide-SVMP fusion protein yields in the media remained too low to
170 progress to purification.

171 Next, we tested expression of complete SVMP zymogens, where the entire prodomain
172 including propeptide is fused N-terminally to the MP domain (Fig. 2d) adopting a compact
173 structure as predicted by AlphaFold 3 (*31*) with high inter-chain predicted Template Modelling
174 (ipTM) and predicted TM scores (Fig. S2). Cells expressing PI, PII and PIII SVMPs as
175 zymogens showed clearly improved cell viability, remaining above 60% on day 4 of expression
176 (Fig. 2h). PIII SVMP zymogen was harvested on day 4 to avoid additional cell death and lysis.
177 In contrast, the cells expressing PI and PII SVMPs remained ~75% viable on day 5 of
178 expression when the SVMPs were harvested. Notably, the zymogen-expressing cells had
179 considerably higher YFP readings as compared to the cells previously expressing mature PI
180 and PIII SVMPs, and no loss of YFP fluorescence over time was observed (Fig. 2i). Western
181 blot analysis confirmed the presence of PI, PII and PIII zymogens in cell extract and lysate;
182 and zymogen protein was also detected in the media fraction, indicating successful secretion
183 (Fig. 2j). We conclude that SVMPs require the full-length N-terminally fused prodomain to
184 ensure enzyme latency is maintained, and to allow for significant amounts of protein to be
185 produced and secreted when recombinantly expressed using a baculovirus/insect cell system.

186 **SVMP zymogens can be produced in mg amounts.**

187 Following secretion of the SVMP zymogens into the media, a three-step purification was
188 performed. Firstly, cells were pelleted by centrifugation, and the media containing secreted
189 proteins were passed through a HiTrap IMAC column for metal affinity purification to enrich
190 the secreted SVMPs from the comparatively large culture media volume. SVMPs were eluted
191 using imidazole. Fractions containing SVMP zymogen were dialyzed and further purified by
192 anion exchange chromatography (IEX), followed by size exclusion chromatography (SEC).
193 SVMP zymogens generally eluted in one prominent peak in SEC (Fig. 3).

194 Notably, dialysis following IMAC affinity purification of PI SVMP resulted in self-cleavage of
195 the zymogen as evidenced by a downward shift of the PI protein band in the SDS gel from 55
196 kDa to 45 kDa before and after dialysis, respectively (Fig. S3a). Western Blot analysis
197 indicated a loss of the His-tag after dialysis (Fig. S3b). The protein was confirmed to be PI
198 SVMP by mass spectrometry (Fig. S3c). This auto-activation of PI SVMP is likely due to
199 residual metal ions in the insect cell media and buffers, trace metal ions leaching off the resin
200 during IMAC purification, and/or a change in pH from the cell culture medium at pH 6 to the
201 purification buffer at pH 8 - the lower pH of the medium being similar to that of the venom
202 gland (pH 5.4), which helps maintain enzyme latency (*32*). The PI SVMP zymogen without the

203 C-terminus (including the Avi-tag and His-tag), eluted from the SEC column in one peak at
204 14.8 ml, corresponding to a calculated molecular weight (MW) of ~50 kDa which agrees with
205 the predicted MW for the monomeric zymogen (Fig. 3a). The yield of purified PI SVMP
206 zymogen was 0.63 mg from a 1 L Hi5 insect cell culture.

207 Following observation of the loss of the SVMP PI C-terminus during purification, a new protein
208 construct was designed with the Avi- and His-tags fused C-terminally to the observed
209 proteolytic degradation site as suggested by MW loss seen by SDS-PAGE and based on
210 AlphaFold 2 models (*30*), giving rise to a shorter construct named PIΔC. In fact, this new C-
211 terminus of the MP domain aligns with that of fully characterized PI SVMPs (*33-35*). During
212 PIΔC IMAC affinity purification, the zymogen (predicted MW: 45.4 kDa) underwent partial
213 activation, resulting in cleavage between the MP (theoretical MW: 26.2 kDa) and prodomain
214 (theoretical MW: 19.3 kDa) (Fig. S4a). Subsequent IEX allowed for the isolation of a small
215 amount of PIΔC MP domain alone, however the bulk of the PIΔC MP remained bound to the
216 prodomain, forming a stable complex despite cleavage. The PIΔC MP domain alone eluted
217 from the SEC column at a MW of ~29 kDa, corresponding to the MW expected for the
218 monomeric MP domain (Fig. S5a). The PIΔC metalloproteinase in complex with the prodomain
219 eluted from the SEC column in a different peak corresponding to a MW of ~48 kDa, confirming
220 that the cleaved prodomain and MP domain form a stable assembly with a 1:1 stoichiometry
221 (Fig. S5b). The yield of PIΔC was 0.44 mg for the MP domain and 3.25 mg for the MP with
222 non-covalently bound prodomain from a 1 L Hi5 insect cell culture.

223 The PII SVMP zymogen was purified as intact zymogen and did not undergo any
224 (self-)cleavage throughout purification (Fig. 3b). In SEC, a small amount of protein eluted in
225 the void volume, likely due to the very high concentration of PII zymogen when loaded onto
226 the column, possibly causing some aggregation. The majority of PII SVMP zymogen eluted
227 with a small peak corresponding to ~198 kDa (p2) and a large, sharp peak corresponding to
228 ~84 kDa (p3). SDS-PAGE analysis with non-reducing loading dye suggests that peak p2
229 corresponds to a PII zymogen dimer (Fig. S6a, b). Peak p3 corresponds to the monomeric PII
230 SVMP zymogen, which has a predicted MW of 56 kDa, in agreement with its elution volume
231 in SEC. The yield of PII SVMP zymogen was 8.3 mg (peak 3) from a 1 L Hi5 insect cell culture.

232 The PIII SVMP zymogen underwent partial activation during the purification process, similar
233 to that of PIΔC SVMP. This was observed following elution from the IMAC column (Fig. S4b)
234 and resulted in the presence of three bands in SDS-PAGE (Fig. 3c), corresponding to the PIII
235 zymogen (predicted MW 70.2 kDa), mature PIII SVMP (MP domain, disintegrin-like domain
236 and cysteine-rich domain) with a predicted MW of 50.6 kDa, and the prodomain with a MW of
237 19.6 kDa. Interestingly, despite the processing of some PIII molecules, the protein still eluted
238 in one peak from the SEC, at a MW of ~108 kDa based on the elution volume. This indicates

239 that the prodomain again remains associated with the mature SVMP following cleavage, as
240 previously observed for the PIΔC SVMP (Fig. S4a). The yield of the PIII SVMP was 2.2 mg
241 from a 1 L Hi5 insect cell culture.

242 We observed a difference in the calculated MW based on SEC elution volume (~108 kDa) and
243 the predicted MW (70 kDa) for the PIII SVMP zymogen. Similarly, the PIII zymogen and mature
244 PIII SVMP both run at a higher-than-expected MW on SDS-PAGE (~80 kDa and ~60 kDa,
245 respectively). This extra size could be attributed to the presence of N-glycans on the mature
246 SVMP. The NetNGlyc 1.0 server predicts 2 glycosylation sites in the mature PIII SVMP (*36*),
247 and we therefore tested all purified SVMP zymogens for glycosylation using Peptide:N-
248 glycosidase F (PNGase F) (Fig. S7). The bands corresponding to PI and PII SVMPs did not
249 change in the presence of PNGase F. However, we observed a downward shift in the MW of
250 the bands corresponding to the PIII zymogen and mature PIII SVMP protein in SDS-PAGE
251 following treatment with PNGase F. De-glycosylation of PIII proteins produced bands at ~77
252 kDa and ~57 kDa, closer to their predicted MWs (Fig. S7c). We conclude that the PIII SVMP
253 we produced is highly likely to be glycosylated, and possibly not all of the glycosylation could
254 be removed by PNGase F treatment.

255 In conclusion, by using the protocol we have developed, we can produce highly purified
256 recombinant SVMP zymogens, each in mg quantities per Liter expression culture.

257 **Co-expression of protein disulfide isomerases does not improve SVMP zymogen yields**
258 **or folding.**

259 Transcriptomic studies have shown that snake venom glands overexpress several chaperones
260 alongside venom toxins, in particular protein disulfide isomerases (PDI), heat shock proteins
261 and calreticulin (*37*). These chaperones are expected to be essential for the correct folding of
262 complex, disulfide-rich toxins. In particular, PDIs assist in the formation, breakage and
263 rearrangement of disulfide bonds, stabilizing the proteins. Successful folding of venom
264 peptides aided by PDI was previously demonstrated for marine cone snails (*38*). Furthermore,
265 overexpression of PDI during recombinant protein expression has also been shown to
266 increase overall protein yield (*39*). Therefore, we hypothesized that co-expression of SVMPs
267 with PDI could increase SVMP protein yields due to enhanced disulfide bond formation,
268 enabling more protein to be correctly folded and secreted, potentially reducing protein
269 aggregation. To test our hypothesis, we selected two PDIs, a human PDI (UniProt ID: P07237)
270 and a snake PDI (from *Echis ocellatus*) (*25*), which is overexpressed in venom gland tissue.
271 We generated expression cassettes for human PDI or snake PDI alongside our SVMPs and
272 used Cre-LoxP recombination to integrate these cassettes into our SVMP expression
273 constructs (*40*).

274 Successful co-expression of human PDI or snake PDI, alongside our SVMPs, was confirmed
275 by Western Blot and mass spectrometry analysis (Fig. S8a). Contrary to our expectation,
276 however, co-expression of PII and PIII SVMP zymogens with these PDIs did not improve the
277 yield of SVMP zymogens: The SEC chromatograms for PII SVMP zymogens after IMAC and
278 IEX purification expressed in the presence and absence of co-expressed PDI aligned perfectly,
279 with identical peak areas (Fig. S8b). Similarly, the SEC chromatograms for purified PIII SVMP
280 zymogens are virtually identical in the presence or absence of PDIs (Fig. S8c).

281 We conclude that, contrary to expectations, PDI overexpression in insect cells does not
282 enhance the expression and/or folding of our SVMP zymogens and therefore did not result in
283 a noticeable improvement in yield.

284 **Auto-activation of SVMP zymogens reveals cleavage of the prodomains, the PII**
285 **disintegrin domain and PIII prodomain degradation.**

286 Cleavage of the prodomain in native zymogens is thought to result in the removal of the
287 propeptide from the active site, and therefore activation of the enzyme. SVMP zymogens are
288 theoretically inactive enzymes, maintained in this state by the cysteine switch mechanism of
289 the propeptide within the prodomain (Fig. 2d). Zymogens are activated by an unknown
290 mechanism in venom, removing the propeptide from the active site, rendering it accessible to
291 substrates, with Zn^{2+} as an essential cofactor. We thus hypothesized that activation of our
292 purified zymogens could be achieved by addition of Zn^{2+} ions. We optimized the Zn^{2+}
293 concentration for activation for each SVMP (Fig. 3d-f). Incubation with Zn^{2+} ions was carried
294 out at 37ºC for 18 hours.

295 The PI SVMP zymogen could be close to completely activated by 750 μM $ZnCl_2$ (Fig. 3d).
296 When analysed by SDS-PAGE, the ~45 kDa band corresponding to the zymogen mostly
297 disappears, and two lower MW bands of ~23 kDa and ~26 kDa appear, corresponding to the
298 prodomain and MP domain, respectively. The two proteins could not be separated under the
299 native conditions of SEC, indicating that the prodomain remains stably bound to the MP
300 domain, despite cleavage (as observed for PIΔC, Fig. S5b). Separation of the MP and
301 prodomain has occurred during SDS-PAGE, however, due to the denaturing and thiol-reducing
302 conditions used. AlphaFold 2 generated models (*30*) (Fig. 2d) suggest the prodomain is
303 located on the opposite side of the MP domain, distal from the active site. Thus, bound
304 prodomain is not expected to interfere with the ability of the metalloproteinase to bind and
305 cleave substrates, once the propeptide has been detached from the active site. It is interesting
306 to note that the C-terminal part of the PI SVMP zymogen was cleaved during buffer exchange
307 by dialysis while the zymogen was still intact (Fig. S3a) and assumed to be inactive. The
308 observed C-terminal cleavage could be due to a few auto-activated PI SVMPs or due to
309 contaminating proteases from insect cells still present in the affinity purified protein fractions.

310 The truncated PI∆C SVMP construct was almost completely cleaved into mature protein
311 during purification, however this protein was not fully active in activity assays (data not shown).
312 For full activity, the PI∆C SVMP was incubated with 300 µM $ZnCl_2$. Despite complete cleavage
313 of the zymogen, the resulting prodomain and MP domain could not be separated, as was the
314 case for the full-length PI, and, thus, no MP was isolated from this construct either (Fig. S9).
315 Because this PI∆C SVMP corresponds better to the processed, more native version of PI
316 SVMP protein, PI∆C was used in all further activity assays and is referred to as PI SVMP from
317 here on.

318 The PII SVMP zymogen was completely activated by 750 µM $ZnCl_2$ (Fig. 3e). Notably, when
319 analysed by SDS-PAGE, a clear separation of prodomain and mature protein was not
320 observed. The band migrating at ~40 kDa corresponds to MP and disintegrin (confirmed by
321 Western blot, Fig. S6c). This band disappears with higher concentrations of Zn^{2+} and/or longer
322 incubation times. The band migrating at ~8 kDa is thought to correspond to the processed
323 disintegrin domain but could not be confirmed by Western blot due to loss of C-terminal tags
324 during activation. After incubation for 1 week, only the 8 kDa and 23 kDa bands remained (Fig.
325 3e). Based on apparent MW, these bands correspond to the disintegrin and prodomain,
326 respectively. In summary, PII SVMP has undergone further processing to remove the tags and
327 disintegrin from the MP domain, and the MP domain appears to be unstable over time.

328 The PIII SVMP zymogen was completely activated by the addition of 150 µM $ZnCl_2$ (Fig. 3f)
329 as evidenced by the disappearance on SDS-PAGE of the ~77 kDa band corresponding to the
330 zymogen. Instead, the band strengthened at ~60 kDa corresponding to the mature SVMP (MP
331 domain plus disintegrin-like domain and cysteine-rich domain) together with a band at ~25 kDa
332 corresponding to the prodomain. Notably, at higher concentrations of Zn^{2+}, the C-terminal tags
333 and the prodomain band are degraded by the PIII SVMP.

334 We conclude that all SVMP zymogens studied can auto-activate by incubation with Zn^{2+},
335 leading to cleavage of the prodomain from the zymogen. In the case of PI∆C and PIII SVMPs
336 the prodomain remains associated with the SVMP at low Zn^{2+} concentrations. After Zn^{2+}
337 activation, the C-terminal tags and the PIII prodomain are degraded by the activated SVMPs,
338 and in the case of PII SVMP, further proteolysis occurs into the constituent parts.

339 **Casein and fibrinogen degradation assays demonstrate SVMP activity.**

340 Degradation of casein is a general SVMP activity assay that is used in functional assays for
341 all SVMP classes (*23*). SVMP zymogens were supplemented with optimal concentrations of
342 $ZnCl_2$ for SVMP activation (Fig. 3d-f) and incubated with 0.525 µg/µl (~23 µM) casein overnight
343 at 37°C. The degradation of casein was analysed by SDS-PAGE; indicated concentrations
344 relate to input SVMP zymogen concentrations (Fig. 4a-f). The PI SVMP degraded casein (Fig.

345 4a); activity was observed when adding 73 nM PI and complete degradation of casein
346 occurred at the addition of 1.17 μM PI. The PII SVMP exhibited weak activity against casein
347 (Fig. 4b), which may be due to the self-degradation of the MP domain observed during Zn^{2+}
348 activation (Fig. 3e). Casein degradation was observed when adding 1.36 μM PII, as evidenced
349 by the emergence of lower MW bands (Fig. 4b). The PIII SVMP was active against all casein
350 chains (Fig. 4c), with activity seen from concentrations as low as 21 nM PIII, and complete
351 digestion of casein was observed with 343 nM PIII.

352 Next, we performed fibrinogen degradation assays followed by SDS-PAGE analyses (Fig. 4d-
353 f). None of our recombinant SVMPs had strong activity against the γ chain of fibrinogen, as is
354 usually the case with SVMPs (*35*). However, PI, PII and PIII SVMPs degraded Aα and Bβ
355 chains of fibrinogen to different extents:

356 The majority of PI SVMP activity is directed against the Aα chain of fibrinogen (Fig. 4d), with
357 the lowest amount of enzyme tested (73 nM). At higher concentrations of PI (585 nM), activity
358 towards the Bβ chain was also observed. Therefore, PI SVMP can be classified as an
359 alpha/beta fibrinogenase, with a preference for the Aα chain. PII SVMP caused removal of
360 fibrinopeptide B (FpB) from the Bβ chain (Fig. 4e) at a concentration of 134 nM. At higher
361 concentrations (268 nM or more), the Aα chain was also degraded. Thus, PII SVMP is an
362 alpha/beta fibrinogenase with a preference for the Bβ chain. PIII SVMP degraded the Aα chain
363 of fibrinogen at the lowest concentration of PIII tested, 21 nM (Fig. 4f). When supplementing
364 85 nM PIII or more, the band at 60 kDa corresponding to the Bβ chain disappears as well.
365 Thus, we classify PIII SVMP as an alpha/beta fibrinogenase, with a preference for the Aα chain.

366 As described above, we also expressed recombinant PII and PIII SVMPs in the presence of
367 co-expressed human or snake PDI, but without an improvement in yields (Fig. S8a-c). It
368 remained possible, however, that the activity of these SVMPs could have been enhanced by
369 the co-expression of the PDIs resulting in improved protein folding, e.g. through optimized
370 disulfide bond formation. When tested against fibrinogen, however, the activities of the
371 different SVMPs remained unchanged by PDI co-expression (Fig. S8d,e).

372 To summarize, all recombinant SVMPs (PI, PII, PIII) degraded casein, confirming their activity.
373 They also degraded the alpha and beta chains of fibrinogen in a fibrinogenolytic manner, rather
374 than cleaving fibrinopeptides in a thrombin-like manner.

375 **Auto-activated PIII SVMP shows high substrate affinity and catalytic efficiency.**

376 We next tested if the SVMPs cleave a quenched fluorogenic substrate, ES010 (R & D Systems)
377 which is commonly used to study SVMPs (*41*) and matrix metalloproteinases (*42*) for small
378 molecule therapeutic discovery. PIII SVMP was able to cleave the Gly-Leu bond in ES010
379 (Fig. 4g). In contrast, SVMPs PI and PII did not effectively cleave this substrate under the

380 conditions tested (not shown). Using 20 nM zymogen concentration (corresponding to 90 ng
381 PI, 110 ng PII and 140 ng PIII enzyme concentration/well), the reaction was carried out at 25°C
382 in 50 mM Tris, 300 mM NaCl, pH 7.5 in a 96 well plate and not stirred. The rate of reaction
383 (monitored by fluorescence increase) was plotted against varying substrate concentrations
384 (ranging from 0 μM to 180 μM), and a Michaelis-Menten curve was calculated (Fig. 4g). The
385 low K_M of 19.6 μM indicates a high binding affinity of the PIII SVMP for the ES010 fluorogenic
386 substrate. The high catalytic efficiency (k_{cat}/K_M) of 3.26 x10^7 $M^{-1}s^{-1}$ further suggests that the
387 PIII SVMP is highly effective and specific in processing this substrate. For comparison, a
388 k_{cat}/K_M value of 4,471 $M^{-1}s^{-1}$ was reported for matrix metalloproteinase MMP10 for an ESO10-
389 derived peptide (*43*), and k_{cat}/K_M values of 30,000 $M^{-1}s^{-1}$ for a triple-helical peptide for MMP-2
390 (*44*). Together, these parameters demonstrate that the recombinant PIII SVMP exhibits both
391 strong substrate affinity and high catalytic efficiency toward a prototypical PIII SVMP substrate.

392 **Native and recombinant PI SVMP exhibit the same substrate specificity in insulin B**
393 **degradation assays.**

394 Next, we assayed the activity of SVMPs PI and PIII against insulin B, a test substrate used
395 previously in SVMP characterization (*13*). Degradation of insulin B at multiple sites was
396 visualized by RP-HPLC. PI and PIII showed distinct insulin B degradation patterns indicating
397 different sequence specificities and cleavage sites. PIII SVMP cleaves insulin B into 6 products
398 (Fig. 4h). PI SVMP cleaves insulin B into 5 products (Fig. 4i). Importantly, this PI SVMP can
399 also be readily purified from *Echis ocellatus* venom. Therefore, we could compare insulin B
400 cleavage by our recombinant PI SVMP with insulin B cleavage by the native source-purified
401 PI enzyme. Identical degradation products of insulin B were observed. Thus, our recombinant
402 PI SVMP is active and has the same substrate specificity as the native enzyme from venom,
403 underscoring that our recombinant expression strategy leads to native-like SVMPs,
404 compellingly validating our approach.

405 **PII zymogen and activated PII SVMP inhibit platelet aggregation.**

406 Some haemorrhagic SVMPs can disrupt cell adhesion and prevent haemostasis by interfering
407 with platelet aggregation (*45*). SVMPs with either a disintegrin (PII), or disintegrins-like domain
408 (PIII) can inhibit platelet aggregation through a motif found in these domains. Most commonly,
409 this corresponds to a RGD sequence, which binds integrins. Binding of disintegrin to integrin
410 $\alpha_{IIb}\beta_3$ can be measured through inhibition of ADP-induced platelet aggregation whereby
411 turbidity is determined by flow cytometry (Fig. 5a). Platelet aggregation was close to
412 completely inhibited by the PII SVMP, in both the zymogen and mature, Zn^{2+}-activated enzyme
413 form confirming that the disintegrin is active. Based on our results, the presence of the
414 prodomain in the zymogen has no inhibitory effect on the RGD-containing disintegrin domain,
415 as anticipated. In comparison, the PIII SVMP did not inhibit ADP-induced platelet aggregation

416 (Fig. 5a). Instead of an RGD motif, this PIII SVMP has a divergent 'RSECD' motif in its
417 disintegrin-like domain which most likely does not interact with integrin $\alpha_{IIb}\beta_3$. We conclude
418 that our recombinant PII SVMP inhibited platelet aggregation, confirming disintegrin activity in
419 the context of both the zymogen and also the activated PII SVMP.

420 **PIII SVMP has no pro-coagulant activity in thrombin clot time assays.**

421 Thrombin clot time assays measure the time required for thrombin to convert fibrinogen to
422 fibrin, leading to clot formation. This assay is used in the clinic to highlight abnormalities in
423 fibrinogen and fibrin clot formation. In our assays, thrombin was replaced with each SVMP to
424 identify the thrombin-like activity of the enzyme. The assay measures turbidity, which is plotted
425 against time. The first and second derivatives are plotted on the same graph, and the
426 maximum rate of change of turbidity (the peak in the 2nd derivative) indicates the time of clot
427 formation. When thrombin is added, fibrin clot formation requires 16.5 seconds (Fig. 5b). As a
428 positive control and example of pro-coagulant SVMPs, thrombin was replaced with native PIII
429 SVMPs purified from *Echis ocellatus* venom. Fibrin clot formation occurs in 28.1 seconds in
430 the presence of *Echis ocellatus* PIII SVMPs (Fig. 5c), confirming clot formation and pro-
431 coagulation activity. However, when replaced with the recombinant PIII SVMP (from *Echis*
432 *carinatus sochureki*) no clot formation occurs (Fig. 5d). This shows that our recombinantly
433 produced PIII SVMP has no pro-coagulant activity.

434 **PI and PIII SVMPs are cytotoxic.**

435 HaCaT cells, immortalized human keratinocyte cells commonly used in dermatological,
436 toxicological and cancer research, were incubated with PI, PII and PIII SVMPs for 24 hours
437 (100 µg/ml SVMP in standard medium). Cytotoxicity was monitored using the MTT (3-(4,5-
438 dimethylthiazol-2-yl)-2,5-diphenyltetrazolium bromide) assay (*46*). The resulting percentage
439 of cell viability was calculated as described in the Methods part. At the tested concentration,
440 PII SVMP showed minimal cytotoxicity (Fig. 5e). However, PI and PIII SVMPs were more
441 cytotoxic, with cell viability decreasing by 40% and 50% after 24 hours, respectively (Fig. 5e).
442 The cytotoxic effect of our PIII SVMP (*Echis carinatus)* (100 µg/ml*)* is comparable to that of
443 crude *Echis carinatus* venom on HEK 293T cells, which induces 63% cytotoxicity with 100
444 µg/ml venom after 3 hours (*47*). Published IC_{50} values for HaCaT cells treated with whole
445 venom for 24 hours fall between 10 and 100 µg/ul (*48*), however it is important to highlight the
446 distinction between the complex cocktail of toxins found in venom and the homogenous,
447 purified SVMP evaluated in this study.

448 **DISCUSSION**

449 The characterization of SVMP toxins, critical for effective bioprospecting and the discovery of
450 snakebite therapeutics, is severely hampered by difficulty in isolating the native proteins from
451 venom. Here, we established a generic protocol for efficient recombinant production of the
452 three structurally diverse classes of SVMPs, which overcomes this obstacle. We demonstrate
453 expression of PI, PII and PIII SVMP zymogens from *Echis* species in high quality and quantity
454 using the MultiBac baculovirus/insect cell expression system.

455 Based on transcriptomic data from *Echis* venom gland (*25*), we hypothesized that co-
456 expression of SVMPs with human or snake PDI would aid their proper folding, ensuring the
457 multiple disulfide bonds were correctly formed and thus improving yields and/or activity of the
458 SVMPs. However, co-expression of either a snake PDI, or a commonly used human PDI,
459 neither improved protein yields nor enzyme activity. We conclude that the endogenous insect
460 cell PDIs are sufficient for SVMP folding in our setup. Alternatively, a combination of different
461 chaperones may be required for further boosting SVMP production.

462 In SVMP zymogens, the highly conserved propeptide sequence which blocks the active site
463 of the MP domain, is clamped in place by the N-terminal prodomain. It should be noted that
464 despite expression as a zymogen, residual cytotoxicity was still observed, evident by the
465 decrease in cell viability throughout expression and reduction in the amount of co-expressed
466 YFP fluorescence due to cell lysis (Fig. 2). In agreement with this observation, PI and PIII
467 SVMPs were able to partially activate themselves, resulting in the presence of three
468 characteristic bands in Coomassie-stained SDS-gels – the zymogen, mature SVMP and
469 prodomain. We speculate that this auto-cleavage could be due to the SVMP active site
470 accreting divalent metal ions from the media and buffers used. Additionally, it is likely that the
471 change in pH from 6 (expression) to 8 (purification) allows the activation of SVMPs, as is the
472 case when venom is released from the venom gland (pH 5.4) into the victim (pH 7.4) during
473 envenoming (*32*).

474 Of note, despite the self-cleavage of the PI and PIII zymogens, the majority of the mature
475 SVMP protein remained associated with the prodomain. Interestingly, this did not affect the
476 activity of the SVMPs. According to AlphaFold 2 structure predictions, the prodomain is located
477 on the side of the MP domain which is opposite from the active site. Upon activation, cleavage
478 of the prodomain releases the propeptide from the active site. This renders the Zn^{2+} ion in the
479 active site free to interact with a substate. In agreement, we observe that the SVMPs are active
480 even if the prodomain, now no longer covalently linked to the SVMP, remains bound to the MP
481 domain (Fig. 3c, Fig. S4).

482 SVMP zymogens additionally undergo further post-translational processing: The PI SVMP
483 construct described here was based on transcriptomic data and corresponds to the UniProt
484 sequence ID: Q2UXQ3. During purification, it underwent C-terminal truncation by ~10 kDa,
485 leading to a smaller protein which corresponds closely to previously characterized PI SVMPs
486 (*33-35*). Additionally, we observed a general trend of loss of C-terminal tags during purification,
487 activation and subsequent activity assays for all three SVMP classes.

488 SVMP zymogens from all three classes could be auto-activated by the addition of Zn^{2+} ions.
489 While some PI SVMP was processed during purification, any remaining PI zymogen could be
490 cleaved into the mature SVMP and prodomain by incubation with Zn^{2+}. The PII zymogen could
491 be activated by the same means, although there was no clear separation into prodomain and
492 mature protein. Instead, we observed two bands corresponding to the disintegrin and
493 prodomain after prolonged incubation with Zn^{2+} (Fig. 3e). It is unlikely that the observed
494 disappearance of the MP domain is due to misfolding because the PII zymogen is well
495 expressed with high yields (9-10 mg/L culture) in insect cells and eluted in two clean peaks in
496 SEC corresponding to a monomer and dimer, respectively. In the case of misfolding, we would
497 have expected aggregation and/or degradation during purification, and we would not expect
498 to see degradation of the zymogen in SDS-PAGE analysis only after addition of Zn^{2+} which
499 activates the metalloproteinase (Fig. 3e). Notably, the disintegrin domain of this PII has 100%
500 sequence identity to ocellatusin, a short, monomeric disintegrin and major component of *Echis*
501 *ocellatus* venom (*49*). Previous studies have identified a discrepancy between the amounts of
502 ocellatusin and its PII SVMP precursor in the venom, whereby ocellatusin represents 3.9%,
503 and the PII SVMP less than 0.1% of venom proteins (*3*). In summary, the disintegrin is likely
504 liberated from this PII SVMP and is the more pathogenic component of the SVMP, causing
505 inhibition of platelet aggregation (Fig. 5a). In contrast, the PII-derived metalloproteinase
506 domain is unstable and therefore requires high toxin concentrations to elicit proteolytic activity
507 in our activity assays (Fig. 4b, 4e).

508 The recombinant PIII zymogen was fully auto-activated in our experiments by the addition of
509 Zn^{2+} ions (Fig. 3f). Interestingly, this PIII SVMP was able to degrade its prodomain despite the
510 latter initially remaining bound to the mature protein according to SEC (Fig. 3c). This agrees
511 with the finding that prodomains, which are highly conserved in SVMPs, are rarely identified
512 in the venom proteome (*50*), suggesting that all prodomains might eventually be fully degraded
513 by venom proteases including PIII SVMPs.

514 Activated recombinant SVMPs were active against bovine casein, a general protease
515 substrate (Fig. 4a-c). PI and PIII exhibited strong activity, degrading all bands, while PII was
516 significantly less active, requiring much higher enzyme concentrations. This agrees with our
517 previous observation that bands corresponding to the MP-disintegrin protein or the MP domain

518 alone after activation with Zn^{2+} (Fig. 3e) are absent in SDS-PAGE, indicating that the MP
519 domain is likely unstable.

520 Fibrinogen degradation assays are particularly relevant for SVMPs and indicate their potential
521 haemotoxic activity (Fig. 4d-f). The 340 kDa fibrinogen glycoprotein is made up of three pairs
522 of polypeptide chains, which lead to three groups of distinct bands when analysed by reducing
523 SDS-PAGE: the Aα (70-75 kDa), Bβ (65 kDa) and γ (50 kDa) chains. In contrast to the
524 endogenous serine protease thrombin, which cleaves fibrinopeptides A and B off the Aα and
525 Bβ chains, causing self-polymerization into fibrin fibres and formation of blood clots (*51*), the
526 PI, PII, and PIII SVMPs studied here caused a fuller degradation of fibrinogen (Fig. 4d-f). All
527 SVMPs were active against both the Aα and Bβ chains of fibrinogen; the PI and PIII showed
528 a preference for the Aα chain and the PII preferentially degraded the Bβ chain of fibrinogen.
529 We conclude that the three SVMPs interfere with clot formation and would thus contribute to
530 an anticoagulant outcome upon envenoming. In agreement, the PIII SVMP cannot cause clot
531 formation in the thrombin clot time assay (Fig. 5d), suggesting it is not an Ecarin-like
532 prothrombin activator, which is typically responsible for procoagulant activity seen in such
533 assays with *Echis* venoms (Fig. 5c).

534 The recombinant PIII SVMP was highly active against a fluorogenic peptide substrate, ES010,
535 showing high affinity and specificity for cleavage of the Gly-Leu bond within the peptide (Fig.
536 4g). In this context, we would like to point out that, enzyme concentrations and kinetics are
537 based on zymogen concentrations, assuming 100% SVMP activation by Zn^{2+} (Fig. 4a-g). If
538 zymogen activations were incomplete or non-linear, our k_{cat}/K_M calculations could either
539 underestimate or overestimate the PIII SVMP's catalytic efficiency (Fig. 4g).

540 The SVMP PIII was also active against insulin B (Fig. 4h), as was SVMP PIΔC (Fig. 4i) which
541 produced identical degradation products to native PI, confirming identical cleavage sites and
542 successful recombinant production of toxin with native-like characteristics, validating our
543 approach.

544 In addition to the proteolytic activity of the MP domain, PII and PIII SVMPs also include a
545 disintegrin or disintegrin-like domain containing a potential integrin binding motif. In platelet
546 aggregation assays, our RGD-containing PII SVMP inhibited ADP-induced platelet-
547 aggregation with and without the prodomain present (Fig. 5a). The RSECD-containing PIII, in
548 contrast, did not inhibit ADP-induced platelet aggregation, but this does not exclude other
549 disintegrin-like activity of this domain.

550 Zymogen expression was previously reported for ADAMs (A Disintegrin and
551 Metalloproteinases) and MMPs (Matrix Metalloproteinases), which are structurally and
552 functionally related to SVMPs. ADAMs and MMPs are involved in cell-cell interactions,

553 ectodomain shedding and degradation of extracellular matrix components respectively (*52*).
554 ADAMs and MMPs have become prominent targets in drug discovery (*53*, *54*). For MMPs,
555 zymogen expression in mammalian and insect cells has been reported and enzyme activation
556 was achieved via 4-aminophenylmercuric acetate or trypsin to remove the prodomain (*55*, *56*).
557 Moreover, ADAMs have been expressed with their prodomain to aid proper folding and latency
558 (*57*, *58*). The ADAMs prodomain has been removed post-translationally, e.g. by co-expression
559 of furin (*59*). Interestingly, in agreement with our PI and PIII SVMP observations, ADAM33
560 zymogen was processed and secreted in *Drosophila* S2 cells, with the prodomain remaining
561 associated with the catalytic domain after purification. The processing was enhanced by
562 addition of cadmium chloride and zinc chloride (*60*). Auto-activation of zymogens by Zn^{2+}
563 incubation alone, however, has not been reported to the best of our knowledge.

564 While ADAMs and MMPs are well characterized in the literature, comparable insights into
565 SVMPs were largely absent to date, due to lack of means for recombinant SVMP protein
566 production. Our generic protocol for recombinant SVMP zymogen production of all three
567 classes overcomes their high cytotoxicity and allows, for the first time, to study auto-activation
568 revealing important differences between the SVMP classes. Furthermore, our protocol will
569 unlock the production of many additional hitherto inaccessible SVMPs, allowing in-depth
570 characterization of their post-translational processing, enzymatic activity, substrate specificity,
571 cyto- and haemotoxicity, and enable the evaluation of potential biomedical applications to
572 develop new diagnostics and treatments for blood clotting disorders. Our study paves the way
573 to engineer existing and new SVMPs for improved and novel applications in haematology,
574 thrombosis and inflammation research and other important areas in which SVMPs can play a
575 crucial role. Importantly, the recombinantly produced, tagged SVMPs can serve as antigens
576 for the future selection and evolution of neutralizing antibodies as a basis for next-generation
577 snakebite treatment to combat snakebite envenomation.

578 **MATERIALS AND METHODS**

579 **SVMP expression construct design**

580 PI, PII and PIII SVMP constructs were designed by fusing an Avi- and His-tag
581 (GGSGLNDIFEAQKIEWHEHHHHHHHH*) to the C terminus of the native SVMP sequences
582 listed on UniProt (RRID: SCR_004426) (PI – Uniprot ID: Q2UXQ3, PII – Uniprot ID:
583 A0A3G1E3U2, PIII – Uniprot ID: E9JG34). The sequences were codon-optimized for
584 *Spodoptera frugiperda*, gene synthesized (Genscript) and inserted into the plasmid
585 pACEBac1 (Geneva Biotech), which acted as the donor in the MultiBac system (*61*). Structure
586 predictions of SVMP zymogens were performed using AlphaFold 3 (*31*) in the presence of a
587 single Zn^{2+}. Per residue predicted Local Distance Difference Test (pLDDT) plots, indicating
588 local confidence, were generated from B-factor values stored in the .cif files. The highest-
589 ranked model among the five predictions was selected for visualization and figure generation
590 using UCSF ChimeraX (RRID:SCR_015872, https://www.cgl.ucsf.edu/chimerax/).

591 Mature SVMP constructs did not include the prodomain, but did contain an N-terminally fused
592 melittin signal sequence (MKFLVNVALVFMVVYISYIYA). Propeptide-SVMP fusions contained
593 an additional N-terminally fused propeptide triplicate and TEV site
594 (GGSPKMCGVTPKMCGVTPKMCGVTENLYFQSN) following the melittin signal sequence.
595 SVMP active site mutants were based on the mature SVMP constructs, but with the active site
596 glutamic acid mutated to aspartic acid and glycine mutated to cysteine (*28*). Zymogen
597 constructs comprised the native signal sequence preceding the native prodomain (which is
598 specific to the SVMP) and the SVMP sequence with a C-terminal Avi-His-tag fusion. PI was
599 found to undergo C terminal processing, the site of which was predicted by modelling using
600 AlphaFold 2 (*30*). PI∆C construct contained the Avi-His-tag fusion following this site.

601 **Recombinant SVMP expression**

602 Each SVMP-containing pACEBac1 plasmid was expressed using the MultiBac
603 baculovirus/insect cell expression system following established protocols (*62*). SVMPs were
604 expressed in Hi5 insect cells at 19°C, in ESF 921 Insect Cell Culture Media (Expression
605 Systems). The cells were monitored throughout expression by measuring YFP fluorescence
606 (encoded in baculoviral genome) and cell viability (by determining percentage of alive cells
607 using Trypan Blue). A control expression of an unrelated, non-toxic protein (E3 ligase) was
608 used as a control for YFP and cell viability measurements. Expression in the presence of
609 Marimastat was tested using a final concentration of 0 μM, 3 μM and 6 μM Marimastat in the
610 cell culture media, which was added alongside the virus (at the start of expression). Cultures
611 were harvested 5 days after infection by centrifugation (1000 xg, 10 minutes), or when the cell

612 viability was 0% if this occurred sooner. The secreted SVMP proteins were purified
613 immediately after harvesting from the supernatant.

614 **Co-expression of SVMPs with protein disulfide isomerase**

615 The PII and PIII SVMPs were additionally co-expressed with human or snake protein disulfide
616 isomerase (PDI) which was incorporated into the plasmid using Cre-lox (*40*). The multigene
617 expression construct was made using PDI-containing pIDC plasmids (Geneva Biotech).
618 pIDC_hPDI and pIDC_sPDI (PDI-insert synthetised by Genscript) as the donor plasmids were
619 fused with SVMP-containing pACEBac1 plasmids as the acceptor plasmid (*40*). SVMP
620 expression was carried out as above.

621 **Recombinant SVMP purification**

622 Clarified media (containing SVMP) was continuously passed through HiTrap IMAC FF 5 ml
623 column (Cytiva) at 2 ml/min, for 18 hours at 4°C using a peristaltic pump. Subsequently, the
624 column was washed with 10 CV High Salt Buffer (50 mM Tris-Cl, 1 M NaCl, pH 8.0) and 10 CV
625 SVMP Buffer (50 mM Tris-Cl, 300 mM NaCl, pH 8.0). After the washing steps, the IMAC
626 column was attached to an AKTA Pure system. The SVMP was eluted from the IMAC column
627 using a gradient of imidazole from 0 mM to 500 mM imidazole in SVMP buffer. Fractions
628 containing SVMP were pooled and dialyzed into SVMP Low Salt Buffer (50 mM Tris-Cl, 50 mM
629 NaCl, pH 8.0). SVMP was further purified by ion exchange chromatography by passing the
630 dialyzed protein through a 5 ml HiTrap Q XL column. Subsequently, the SVMP was eluted
631 from the column by a gradient of 50 mM to 1 M NaCl in SVMP buffer. Fractions containing
632 SVMP were pooled and concentrated to 500 µl (maximum 10 mg/ml). Finally, SVMP was
633 purified by size exclusion chromatography (SEC) using an Superdex 200 increase 10/300 GL
634 column (Cytiva) in SVMP buffer with a flow rate of 0.375 ml/min. Cytiva Gel Filtration
635 Calibration Kits were used to calibrate the column, with elution peaks plotted to generate a
636 standard curve with which to calculate the molecular weights (MWs) of SVMP proteins. Eluted
637 SVMP was concentrated to 0.5 - 2 mg/ml using an Amicon concentrator with appropriate MW
638 cut off. Glycerol was added to 5% before the protein was flash frozen in liquid nitrogen and
639 stored at -80°C.

640 **SVMP deglycosylation assay**

641 Glycosylation of SVMP zymogens was determined by incubation with peptide-*N*-glycosidase
642 F (PNGase F, Promega) to remove N-linked oligosaccharide groups, followed by SDS-PAGE.
643 Briefly, the reaction was carried out with 1-2 µg SVMP diluted in 12 µl water, followed by
644 addition of 1 µl 5% SDS and 1 µl 1 M DTT. Next, the sample was heated at 95°C for 5 minutes
645 to denature the SVMP zymogens. Once cooled at room temperature, 2 µl SVMP Buffer, 2 µl
646 10% NP-40 and 2 µl PNGase F were added. The reaction mix was incubated at 37°C for

647 3 hours. Subsequently, SDS-PAGE sample buffer (reducing) was added, and the samples
648 were analysed by SDS-PAGE. SVMP zymogen deglycosylation was identified by a shift
649 towards lower MW of the SVMP band compared to the band where PNGase F was omitted.

650 **Purification of PIII SVMP fraction from *Echis ocellatus* venom**

651 As a procoagulant control for blood clot time assays, an *Echis ocellatus* SVMP PIII fraction
652 was prepared using SEC. Whole venom (25 mg) was dissolved in 1.5 ml of PBS (25 mM
653 sodium phosphate, 150 mM NaCl, pH 7.2), centrifuged and the supernatant loaded onto a 120
654 ml column of Superdex75 (Cytiva). Proteins were separated in PBS using a flow-rate of 1.0
655 ml/min and the separation was monitored at 280 nm. Two ml fractions were collected and
656 SDS-PAGE was used to determine the fractions containing SVMP PIIIs. These were pooled
657 and shown to be free of serine protease activity using the casein assay (see above) with
658 appropriate inhibitors.

659 **SVMP enzyme activation**

660 To determine optimal activation conditions, SVMP was titrated with 0 – 750 μM $ZnCl_2$, then
661 incubated at 26ºC or 37ºC for 18 hours. Activation was monitored using SDS-PAGE and
662 disappearance of the SVMP zymogen band in Coomassie-stained gels.

663 **Casein and fibrinogen degradation assays**

664 Activated SVMP was titrated into a freshly prepared 20 μl reaction mix containing casein or
665 fibrinogen at a final concentration of 0.525 mg/ml in SVMP Buffer. Final SVMP concentrations
666 ranged from 0 to 2.34 μM (based on SVMP zymogen concentration at the start of the
667 experiment). The negative control contained 5 mM EDTA as an SVMP inhibitor and maximum
668 concentrations of SVMP (PI - 2.34 μM, PII -1.07 and 1.34 μM, PIII - 685 nM). Incubation was
669 carried out at 37ºC for 18 hours. SDS-PAGE sample buffer was added, and the samples were
670 heated to 95ºC to stop the reaction, and the degradation pattern was analysed by reducing
671 SDS-PAGE.

672 **Fluorogenic peptide substrate cleavage assay**

673 The quenched fluorogenic peptide Mca-KPLGL-Dpa-AR-NH_2 (ES010, R&D systems Inc.) was
674 used to kinetically measure SVMP activity, whereby the activated SVMP cleaves the Gly-Leu
675 bond. Cleavage leads to release of the Dpa-containing quencher from the fluorescent Mca-
676 containing fragment. ES010 substrate was diluted in reaction buffer (50 mM Tris-Cl, 300 mM
677 NaCl, pH 7.5) and used in the assay at final concentrations of 0 μM to 180 μM, in 100 μl in a
678 96 well plate. Enzymes were activated with Zn^{2+} (see above) and diluted in reaction buffer
679 before adding 90 ng PI (45 kDa), 112 ng PII (56 kDa) and 144 ng PIII (72 kDa) enzyme to
680 each well, resulting in a final concentration of 20 nM based on the SVMP zymogen
681 concentration at the start of the experiment). Fluorescence was followed for 1 hour at 25ºC

682 using a BioTech Synergy Neo2 instrument, an excitation wavelength of 320 nm and emission
683 wavelength of 405 nm. Measurements were taken in triplicate. Data was plotted using Origin
684 (RRID:SCR_014212, https://www.originlab.com/index.aspx?go=PRODUCTS/Origin) , and a
685 non-linear curve fitted using the Michaelis-Menten function. Origin provided the best-fit values
686 for V_{max} and K_M, and k_{cat} could be calculated by V_{max}/enzyme concentration.

687 **Insulin B degradation assay**

688 Insulin B degradation was determined following the established protocol (*13*), using a final
689 concentration of 0.02 mg/ml insulin B and 0.01 mg/ml activated SVMP, in 50 mM Tris-Cl, 150
690 mM NaCl, 1 mM $CaCl_2$, pH 7.5 (TBS) buffer. Incubation was carried out at 37°C for 120 minutes,
691 then trifluoracetic acid was added to 1% to stop the reaction. The whole sample (= 1 µg insulin
692 B) was analysed by RP-HPLC using a C18 reverse phase column.

693 **Inhibition of ADP-induced platelet aggregation by the PII and PIII SVMPs**

694 The assay was based on the Platelet Activation protocol (BD Biosciences). The following
695 modifications were introduced to the original protocol: Human platelet rich plasma (PRP) was
696 prepared by centrifugation of fresh whole blood from healthy donors at 220 xg for 20 minutes.
697 For each reaction, 10 µl activated SVMP (300 nM final concentration) was added to 70 µl PRP,
698 5 µl ADP (20 µM final concentration) and 15 µl FITC Mouse Anti-Human PAC-1 antibody (BD
699 Biosciences, RRID: AB_2230769). Modified Tyrode's Buffer (134 nM NaCl, 2.9 mM KCl, 0.34
700 nM $Na_2HPO_4.12H_2O$, 12 mM $NaHCO_3$, 20 mM HEPES, 1 mM $MgCl_2$, 5 mM glucose) was used
701 instead of SVMP for a positive control (ADP only). The reaction was incubated for 30 minutes
702 in the dark at 25°C, prior to fluorescence data acquisition (10,000 events) in a BD Accuri C6
703 Plus flow cytometer (excitation – 488 nm). Platelet activation data was normalized accounting
704 for the mean FITC fluorescence of the positive control as 100%, and the mean FITC
705 fluorescence of the negative control (no ADP added to the reaction) as 0%. Experiments were
706 performed in triplicate.

707 **Thrombin / SVMP clot time assay**

708 Experiments were carried out following manufacturer's kit instructions (HemosIL, Thrombin
709 Time 0009758515), using an ACL TOP coagulation analyser using 3.0 U/ml thrombin, 500 ng
710 PIII SVMP pool purified from *Echis ocellatus* venom and 500 ng activated recombinant PIII
711 SVMP. The assay measures the rate of increase in turbidity as the fibrin clot forms. The peak
712 in the rate of change (2nd derivative) is considered to be the point of clot formation.

713 **MTT cell viability assay**

714 MTT assay was based on the methods of Hall *et al.* (*48*). Immortalized human epidermal
715 keratinocytes, HaCaT (Caltag Medsystems, cells derived from a 62-year-old Caucasian male
716 donor's skin epidermis, RRID: CVCL_0038) were seeded (5,000 cells/well, clear-sided 96-well

717 plates) in standard medium (DMEM high glucose with GlutaMAX™ supplemented with 2 mM
718 sodium pyruvate, 100 IU/ml penicillin, 250 µg/ml streptomycin, 10% Fetal Bovine Serum, 1%
719 GlutaMAX™ (Thermo Fisher Scientific, #35050061)), then left to adhere overnight at 37°C, 5%
720 CO_2. The cell line was freshly procured and checked for contamination before the start of the
721 experiment. The next day, the SVMPs treatments (100 µg/ml) were prepared in standard
722 medium, and cells were treated with each prepared solution (100 µl/well, duplicate wells) for
723 24 hours. For this assay, the MTT Cell Viability Assay Kit (Biotium) was used: 10 µl of MTT
724 solution was added to the 100 µl of medium in each well and mixed by tapping gently on the
725 side of the tray. The cells were incubated at 37 °C for 4 hours. 200 µl DMSO was added directly
726 into the medium in each well and pipetted up and down several times to dissolve the formazan
727 salt. The absorbance was measured on BioTek Synergy Neo2 spectrophotometer at 570 nm.
728 The background absorbance was also measured at 630 nm (subtracted background
729 absorbance from signal absorbance to obtain normalized absorbance values). The % of cell
730 viability for each treatment well was calculated as follows with buffer-treated cells as a control
731 (100% viability):

732 $$\frac{Normalised\ abs\ treatment\ well\ - Average\ normalised\ abs\ blank\ wells}{Average\ normalised\ abs\ cell\ control\ wells - Average\ normalised\ abs\ blank\ wells}$$

733

Materials availability

Materials from this study are available from the corresponding authors upon reasonable request.

Acknowledgements

The authors thank all members of the Berger, Schaffitzel and Casewell teams for discussions and support.

ADDITIONAL INFORMATION

Competing interests: The authors declare that they have no competing interests.

Funding

Funder	Grant reference number	Author(s)
European Commission Horizon2020 FET OPEN	899670	C.S., I.B., R.V, N.R.C.
Wellcome Trust	221708/Z/20/Z	C.S, I.B. N.R.C.
UKRI Engineering Biology Mission Award	BB/Y007581/1	C.S, N.R.C.
EC Marie Sklodowska-Curie Fellowship	101149867; EP/Z002613/1	K.H.
Biotechnology and Biological Sciences Research Council, Studentships		I.A.C., S.L.
The funders had no role in study design, data collection, and interpretation, or the decision to submit the work for publication.		

Author contributions

Sophie Hall, methodology, data curation, formal analysis, investigation, writing – original draft; Iara Aimê Cardoso, methodology, data curation, formal analysis; Mark C. Wilkinson, methodology, data curation, investigation formal analysis, writing - original draft; Maria Molina Carretero, Srikanth Lingappa, Bronwyn Rand, Dakang Shen, data curation, investigation; Johara Boldrini-França, methodology, writing – review and editing; Richard Stenner, methodology; Stefanie K. Menzies, methodology; Georgia Balchin, Konrad Kamil Hus, investigation; Renaud Vincentelli, Investigation; Andrew Mumford, supervision, writing - original draft; Nicholas R. Casewell, Supervision, writing - original draft; Imre Berger, conceptualization, methodology, supervision, writing - original draft; Christiane Schaffitzel, conceptualization, supervision, writing - original draft.

Author ORCIDs

Sophie Hall https://orcid.org/0000-0002-3176-6004

Iara Aimê Cardoso https://orcid.org/0000-0002-0288-4706

Mark C. Wilkinson https://orcid.org/0000-0003-3109-6888

Srikanth Lingappa https://orcid.org/0000-0002-0129-5512.

Bronwyn Rand https://orcid.org/0009-0008-0997-6217

Dakang Shen https://orcid.org/0009-0008-5327-1185

Johara Boldrini-França https://orcid.org/0000-0002-9444-7481

Richard Stenner https://orcid.org/0000-0003-0734-8686

Stefanie K. Menzies https://orcid.org/0000-0002-9273-9296

Georgia Balchin https://orcid.org/0009-0009-6944-6004

Konrad Kamil Hus https://orcid.org/0000-0003-2723-3691

Renaud Vincentelli https://orcid.org/0000-0001-9667-0196

Andrew Mumford https://orcid.org/0000-0002-5523-511X

Nicholas R. Casewell https://orcid.org/0000-0002-8035-4719

Imre Berger https://orcid.org/0000-0001-7518-9045

Christiane Schaffitzel https://orcid.org/0000-0002-1516-9760

ADDITIONAL INFORMATION

Supplementary files

The Supplementary Information contains 9 additional Supplementary figures.

Data availability

All data generated or analysed during this study are included in the manuscript and supporting files.

766 **REFERENCES**

767 1. A. L. Oliveira et al., The chemistry of snake venom and its medicinal potential. *Nat. Rev.*
768 *Chem.* **6**, 451-469 (2022). https://doi.org/10.1038/s41570-022-00393-7

769 2. M. A. Bittenbinder et al., Tissue damaging toxins in snake venoms: mechanisms of action,
770 pathophysiology and treatment strategies. *Commun. Biol.* **7**, 358 (2024).
771 https://doi.org/10.1038/s42003-024-06019-6

772 3. S. C. Wagstaff, L. Sanz, P. Juarez, R. A. Harrison, J. J. Calvete, Combined snake
773 venomics and venom gland transcriptomic analysis of the ocellated carpet viper, *Echis*
774 *ocellatus. J. Proteomics* **71**, 609-623 (2009). https://doi.org/10.1016/j.jprot.2008.10.003

775 4. N. R. Casewell et al., Medically important differences in snake venom composition are
776 dictated by distinct postgenomic mechanisms. *Proc. Natl. Acad. Sci. U.S.A.* **111**, 9205-
777 9210 (2014). https://doi.org/10.1073/pnas.1405484111

778 5. T. Tasoulis, G. K. Isbister, A current perspective on snake venom composition and
779 constituent protein families. *Arch. Toxicol.* **97**, 133-153 (2023).
780 https://doi.org/10.1007/s00204-022-03420-0

781 6. A. F. Asega et al., Cleavage of proteoglycans, plasma proteins and the platelet-derived
782 growth factor receptor in the hemorrhagic process induced by snake venom
783 metalloproteinases. *Sci. Rep.* **10**, 12912 (2020). https://doi.org/10.1038/s41598-020-
784 69396-y

785 7. R. M. Kini, C. Y. Koh, Metalloproteases Affecting Blood Coagulation, Fibrinolysis and
786 Platelet Aggregation from Snake Venoms: Definition and Nomenclature of Interaction
787 Sites. *Toxins (Basel)* **8** (2016). https://doi.org/10.3390/toxins8100284

788 8. J. M. Gutierrez, A. Rucavado, T. Escalante, C. Diaz, Hemorrhage induced by snake
789 venom metalloproteinases: biochemical and biophysical mechanisms involved in
790 microvessel damage. *Toxicon* **45**, 997-1011 (2005).
791 https://doi.org/10.1016/j.toxicon.2005.02.029

792 9. J. M. Gutierrez, T. Escalante, A. Rucavado, C. Herrera, J. W. Fox, A Comprehensive View
793 of the Structural and Functional Alterations of Extracellular Matrix by Snake Venom
794 Metalloproteinases (SVMPs): Novel Perspectives on the Pathophysiology of Envenoming.
795 *Toxins (Basel)* **8** (2016). https://doi.org/10.3390/toxins8100304

796 10. G. O. Almeida, I. S. de Oliveira, E. C. Arantes, S. V. Sampaio, Snake venom disintegrins
797 update: insights about new findings. *J. Venom. Anim. Toxins Incl. Trop. Dis.* **29**,
798 e20230039 (2023). https://doi.org/10.1590/1678-9199-JVATITD-2023-0039

799 11. G. W. Moore, Snake Venoms in Diagnostic Hemostasis and Thrombosis. *Semin. Thromb.*
800 *Hemost.* **48**, 145-160 (2022). https://doi.org/10.1055/s-0041-1732465

801 12. J. Slagboom, J. Kool, R. A. Harrison, N. R. Casewell, Haemotoxic snake venoms: their
802 functional activity, impact on snakebite victims and pharmaceutical promise. *Br. J.*
803 *Haematol.* **177**, 947-959 (2017). https://doi.org/10.1111/bjh.14591

13. M. C. Wilkinson et al., Complex compositional and functional diversity of venom metalloproteinases in African puff adders. bioRxiv, 2024.2005.2031.596867 (2025). https://doi.org/10.1101/2024.05.31.596867

14. K. T. Yee, M. Pitts, P. Tongyoo, P. Rojnuckarin, M. C. Wilkinson, Snake Venom Metalloproteinases and Their Peptide Inhibitors from Myanmar Russell's Viper Venom. *Toxins (Basel)* **9** (2016). https://doi.org/10.3390/toxins9010015

15. O. T. Olaoba, P. Karina Dos Santos, H. S. Selistre-de-Araujo, D. H. Ferreira de Souza, Snake Venom Metalloproteinases (SVMPs): A structure-function update. *Toxicon X* **7**, 100052 (2020). https://doi.org/10.1016/j.toxcx.2020.100052

16. A. Pinyachat, P. Rojnuckarin, C. Muanpasitporn, P. Singhamatr, S. Nuchprayoon, Albocollagenase, a novel recombinant P-III snake venom metalloproteinase from green pit viper (*Cryptelytrops albolabris*), digests collagen and inhibits platelet aggregation. *Toxicon* **57**, 772-780 (2011). https://doi.org/10.1016/j.toxicon.2011.02.011

17. M. T. Assakura, C. A. Silva, R. Mentele, A. C. Camargo, S. M. Serrano, Molecular cloning and expression of structural domains of bothropasin, a P-III metalloproteinase from the venom of *Bothrops jararaca. Toxicon* **41**, 217-227 (2003). https://doi.org/10.1016/s0041-0101(02)00279-9

18. A. Jonebring et al., Expression and characterization of recombinant Ecarin. *Protein J.* **31**, 353-358 (2012). https://doi.org/10.1007/s10930-012-9409-6

19. K. Shimokawa, L. G. Jia, X. M. Wang, J. W. Fox, Expression, activation, and processing of the recombinant snake venom metalloproteinase, pro-atrolysin E. *Arch. Biochem. Biophys.* **335**, 283-294 (1996). https://doi.org/10.1006/abbi.1996.0509

20. E. Camacho, T. Escalante, K. Remans, J. M. Gutierrez, A. Rucavado, Site mutation of residues in a loop surrounding the active site of a PI snake venom metalloproteinase abrogates its hemorrhagic activity. *Biochem. Biophys. Res. Commun.* **512**, 859-863 (2019). https://doi.org/10.1016/j.bbrc.2019.03.152

21. C. Bieniossek, T. Imasaki, Y. Takagi, I. Berger, MultiBac: expanding the research toolbox for multiprotein complexes. *Trends Biochem. Sci.* **37**, 49-57 (2012). https://doi.org/10.1016/j.tibs.2011.10.005

22. O. B. Villaflores et al., Easy expression of the C-terminal heavy chain domain of botulinum neurotoxin serotype A as a vaccine candidate using a bi-cistronic baculovirus system. *J. Virol. Methods* **189**, 58-64 (2013). https://doi.org/10.1016/j.jviromet.2012.11.035

23. J. K. A. Macêdo, Fox, J.W., Biological Activities and Assays of the Snake Venom Metalloproteinases (SVMPs). In *Venom Genomics and Proteomics. Toxinology.* (ed. Gopalakrishnakone, P., Calvete, J.) (Springer, 2016). https://doi.org/10.1007/978-94-007-6416-3_21

24. J. Alsolaiss, N. Alomran, L. Hawkins, N. R. Casewell, Commercial Antivenoms Exert Broad Paraspecific Immunological Binding and *In Vitro* Inhibition of Medically Important

842 *Bothrops* Pit Viper Venoms. *Toxins (Basel)* **15** (2022).
843 https://doi.org/10.3390/toxins15010001

844 25. D. Redureau et al., Dual Proteomics Strategies to Dissect and Quantify the Components
845 of Nine Medically Important African Snake Venoms. *Toxins (Basel)* **17** (2025).
846 https://doi.org/10.3390/toxins17050243

847 26. D. C. Tessier, D. Y. Thomas, H. E. Khouri, F. Laliberte, T. Vernet, Enhanced secretion from
848 insect cells of a foreign protein fused to the honeybee melittin signal peptide. *Gene* **98**,
849 177-183 (1991). https://doi.org/10.1016/0378-1119(91)90171-7

850 27. C. Xie et al., Neutralising effects of small molecule toxin inhibitors on nanofractionated
851 coagulopathic *Crotalinae* snake venoms. *Acta Pharm. Sin. B* **10**, 1835-1845 (2020).
852 https://doi.org/10.1016/j.apsb.2020.09.005

853 28. E. Camacho et al., Novel Catalytically-Inactive PII Metalloproteinases from a Viperid
854 Snake Venom with Substitutions in the Canonical Zinc-Binding Motif. *Toxins (Basel)* **8**
855 (2016). https://doi.org/10.3390/toxins8100292

856 29. F. Grams, R. Huber, L. F. Kress, L. Moroder, W. Bode, Activation of snake venom
857 metalloproteinases by a cysteine switch-like mechanism. *FEBS Lett*. **335**, 76-80 (1993).
858 https://doi.org/10.1016/0014-5793(93)80443-x

859 30. J. Jumper et al., Highly accurate protein structure prediction with AlphaFold. *Nature* **596**,
860 583-589 (2021). https://doi.org/10.1038/s41586-021-03819-2

861 31. J. Abramson et al., Accurate structure prediction of biomolecular interactions with
862 AlphaFold 3. *Nature* **630**, 493-500 (2024). https://doi.org/10.1038/s41586-024-07487-w

863 32. S. P. Mackessy, L.M. Baxter, arBioweapons synthesis and storage: The venom gland of
864 front-fanged snakes. *Zoologischer Anzeiger - A Journal of Comparative Zoology* **245**, 147-
865 159 (2006). https://doi.org/10.1016/j.jcz.2006.01.003

866 33. E. F. Sanchez et al., The novel metalloproteinase atroxlysin-I from Peruvian *Bothrops*
867 *atrox* (Jergon) snake venom acts both on blood vessel ECM and platelets. *Arch. Biochem.*
868 *Biophys.* **496**, 9-20 (2010). https://doi.org/10.1016/j.abb.2010.01.010

869 34. C. A. Bello et al., Isolation and biochemical characterization of a fibrinolytic proteinase
870 from *Bothrops leucurus* (white-tailed jararaca) snake venom. *Biochimie* **88**, 189-200
871 (2006). https://doi.org/10.1016/j.biochi.2005.07.008

872 35. C. P. Bernardes et al., Isolation and structural characterization of a new fibrin(ogen)olytic
873 metalloproteinase from *Bothrops moojeni* snake venom. *Toxicon* **51**, 574-584 (2008).
874 https://doi.org/10.1016/j.toxicon.2007.11.017

875 36. R. Gupta, S. Brunak, Prediction of glycosylation across the human proteome and the
876 correlation to protein function. *Pac. Symp. Biocomput.* 310-322 (2002).
877 https://www.ncbi.nlm.nih.gov/pubmed/11928486

878 37. I. L. Junqueira-de-Azevedo et al., Venom-related transcripts from *Bothrops jararaca*
879 tissues provide novel molecular insights into the production and evolution of snake venom.
880 *Mol. Biol. Evol.* **32**, 754-766 (2015). https://doi.org/10.1093/molbev/msu337

881 38. H. Safavi-Hemami et al., Rapid expansion of the protein disulfide isomerase gene family
882 facilitates the folding of venom peptides. *Proc. Natl. Acad. Sci. U.S.A.* **113**, 3227-3232
883 (2016). https://doi.org/10.1073/pnas.1525790113

884 39. T. A. Hsu, S. Watson, J. J. Eiden, M. J. Betenbaugh, Rescue of immunoglobulins from
885 insolubility is facilitated by PDI in the baculovirus expression system. *Protein Expr. Purif.*
886 **7**, 281-288 (1996). https://doi.org/10.1006/prep.1996.0040

887 40. M. Haffke, C. Viola, Y. Nie, I. Berger, Tandem recombineering by SLIC cloning and Cre-
888 LoxP fusion to generate multigene expression constructs for protein complex research.
889 *Methods Mol. Biol.* **1073**, 131-140 (2013). https://doi.org/10.1007/978-1-62703-625-2_11

890 41. G. T. T. Nguyen et al., High-throughput proteomics and *in vitro* functional characterization
891 of the 26 medically most important elapids and vipers from sub-Saharan Africa.
892 *Gigascience* **11** (2022). https://doi.org/10.1093/gigascience/giac121

893 42. A. Azevedo, A. F. Prado, J. P. Issa, R. F. Gerlach, Matrix metalloproteinase 2 fused to GFP,
894 expressed in *E. coli*, successfully tracked MMP-2 distribution in vivo. *Int. J. Biol. Macromol.*
895 **89**, 737-745 (2016). https://doi.org/10.1016/j.ijbiomac.2016.05.013

896 43. P. Schlage, T. Kockmann, F. Sabino, J. N. Kizhakkedathu, U. Auf dem Keller, Matrix
897 Metalloproteinase 10 Degradomics in Keratinocytes and Epidermal Tissue Identifies
898 Bioactive Substrates With Pleiotropic Functions. *Mol. Cell. Proteomics* **14**, 3234-3246
899 (2015). https://doi.org/10.1074/mcp.M115.053520

900 44. W. J. Akers et al., Detection of MMP-2 and MMP-9 activity *in vivo* with a triple-helical
901 peptide optical probe. *Bioconjug. Chem.* **23**, 656-663 (2012).
902 https://doi.org/10.1021/bc300027y

903 45. S. Takeda, H. Takeya, S. Iwanaga, Snake venom metalloproteinases: structure, function
904 and relevance to the mammalian ADAM/ADAMTS family proteins. *Biochim. Biophys. Acta*
905 **1824**, 164-176 (2012). https://doi.org/10.1016/j.bbapap.2011.04.009

906 46. T. Mosmann, Rapid colorimetric assay for cellular growth and survival: application to
907 proliferation and cytotoxicity assays. *J. Immunol. Methods* **65**, 55-63 (1983).
908 https://doi.org/10.1016/0022-1759(83)90303-4

909 47. R. D. Pierce et al., Characterization of crude *Echis carinatus* venom-induced cytotoxicity
910 in HEK 293T cells. *J. Venom Res.* **2**, 59-67 (2011).
911 https://www.ncbi.nlm.nih.gov/pubmed/22331993

912 48. S. R. Hall et al., Repurposed drugs and their combinations prevent morbidity-inducing
913 dermonecrosis caused by diverse cytotoxic snake venoms. *Nat. Commun.* **14**, 7812
914 (2023). https://doi.org/10.1038/s41467-023-43510-w

915 49. J. B. Smith et al., Characterization of a monomeric disintegrin, ocellatusin, present in the
916 venom of the Nigerian carpet viper, *Echis ocellatus. FEBS Lett.* **512**, 111-115 (2002).
https://doi.org/10.1016/s0014-5793(02)02233-0
917

50. A. M. Moura-da-Silva et al., Processing of Snake Venom Metalloproteinases: Generation of Toxin Diversity and Enzyme Inactivation. *Toxins (Basel)* **8** (2016). https://doi.org/10.3390/toxins8060183ou

51. J. W. Weisel, R. I. Litvinov, Fibrin Formation, Structure and Properties. *Subcell. Biochem.* **82**, 405-456 (2017). https://doi.org/10.1007/978-3-319-49674-0_13son

52. S. Takeda, ADAM and ADAMTS Family Proteins and Snake Venom Metalloproteinases: A Structural Overview. *Toxins (Basel)* **8** (2016). https://doi.org/10.3390/toxins8050155

53. C. M. Overall, C. Lopez-Otin, Strategies for MMP inhibition in cancer: innovations for the post-trial era. *Nat. Rev. Cancer* **2**, 657-672 (2002). https://doi.org/10.1038/nrc884

54. V. J. Craig, L. Zhang, J. S. Hagood, C. A. Owen, Matrix metalloproteinases as therapeutic targets for idiopathic pulmonary fibrosis. *Am. J. Respir. Cell. Mol. Biol.* **53**, 585-600 (2015). https://doi.org/10.1165/rcmb.2015-0020TR

55. Y. Ogata, Y. Itoh, H. Nagase, Steps involved in activation of the pro-matrix metalloproteinase 9 (progelatinase B)-tissue inhibitor of metalloproteinases-1 complex by 4-aminophenylmercuric acetate and proteinases. *J. Biol. Chem.* **270**, 18506-18511 (1995). https://doi.org/10.1074/jbc.270.31.18506

56. R. Vallon, R. Müller, D. Moosmayer, E. Gerlach, P. Angel, The catalytic domain of activated collagenase I (MMP-1) is absolutely required for interaction with its specific inhibitor, tissue inhibitor of metalloproteinases-1 (TIMP-1). *Eur. J. Biochem.* **244**, 81-88 (1997). https://doi.org/10.1111/j.1432-1033.1997.00081.x

57. G. C. Jones, M. N. Vankemmelbeke, D. J. Buttle, Expression of recombinant ADAMTS in insect cells. *Methods Mol. Biol.* **622**, 83-98 (2010). https://doi.org/10.1007/978-1-60327-299-5_5

58. A. Chavaroche et al., Glycosylation of a disintegrin and metalloprotease 17 affects its activity and inhibition. *Anal. Biochem.* **449**, 68-75 (2014). https://doi.org/10.1016/j.ab.2013.12.018

59. E. Wong, T. Maretzky, Y. Peleg, C. P. Blobel, I. Sagi, The Functional Maturation of A Disintegrin and Metalloproteinase (ADAM) 9, 10, and 17 Requires Processing at a Newly Identified Proprotein Convertase (PC) Cleavage Site. *J. Biol. Chem.* **290**, 12135-12146 (2015). https://doi.org/10.1074/jbc.M114.624072

60. W. W. Prosise et al., Protease domain of human ADAM33 produced by *Drosophila* S2 cells. *Protein Expr. Purif.* **38**, 292-301 (2004). https://doi.org/10.1016/j.pep.2004.09.004

61. D. Sari et al., The MultiBac Baculovirus/Insect Cell Expression Vector System for Producing Complex Protein Biologics. *Adv. Exp. Med. Biol.* **896**, 199-215 (2016). https://doi.org/10.1007/978-3-319-27216-0_13

62. D. Sari-Ak et al., VLP-factory and ADDomer: Self-assembling Virus-Like Particle (VLP) Technologies for Multiple Protein and Peptide Epitope Display. *Curr. Protoc.* **1**, e55 (2021). https://doi.org/10.1002/cpz1.55

957 **FIGURES AND LEGENDS**

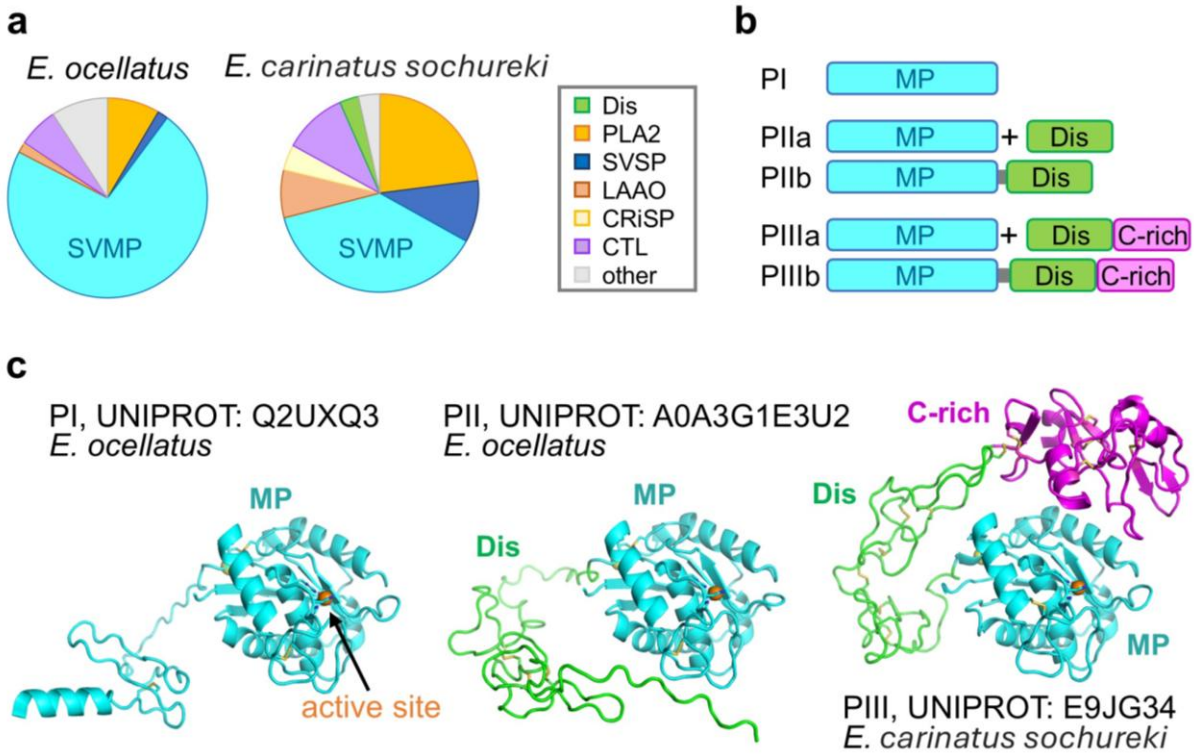

958

959 **Figure 1: SVMP classification and abundance in *Echis* venom.** (**a**) Pie charts displaying
960 *Echis ocellatus* and *Echis carinatus sochureki* venom composition, with SVMP coloured in
961 cyan (*1*). (**b**) Simplified schematic of mature PI, PII and PIII SVMP architecture, showing
962 metalloproteinase domain (MP, cyan), disintegrin domain (Dis, green) and cysteine-rich
963 domain (C-rich, magenta). (**c**) AlphaFold 2 predicted structural models of PI and PII SVMPs
964 from *Echis ocellatus*, and PIII SVMP from *Echis carinatus sochureki*. Domain names and
965 colour coding as in panel b. Zn^{2+} ions (orange) in the active site are shown as spheres.

966

967

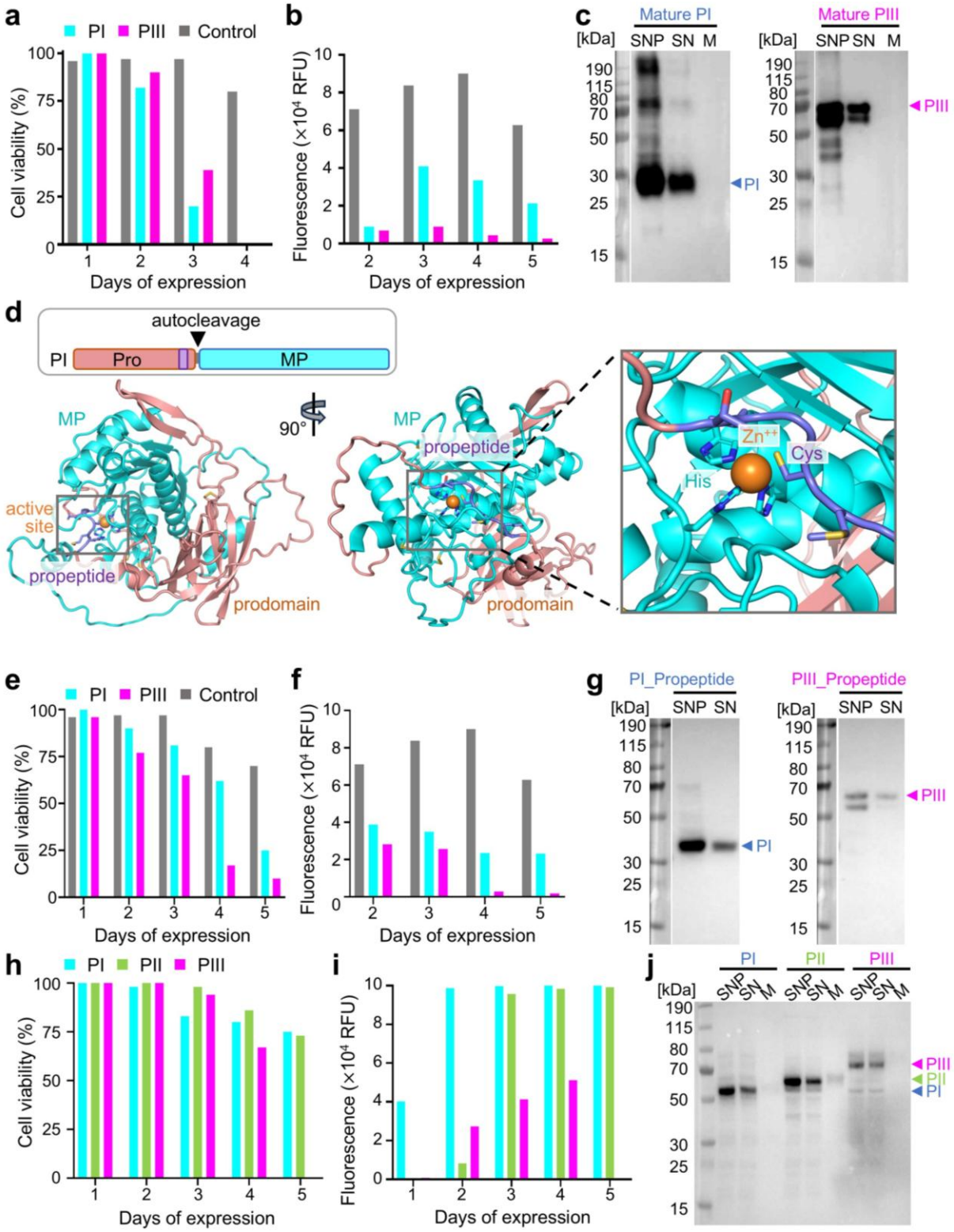

Figure 2: SVMP expression tests to overcome cytotoxicity. Expression of mature SVMPs monitored by (**a**) cell viability, (**b**) YFP fluorescence, (**c**) Western blot analysis of His-tagged protein. (**d**) Above: Schematic of PI SVMP zymogen with N-terminal prodomain (Pro, salmon), propeptide (purple). Below: left: two views of AlphaFold 2 (*30*) prediction of PI zymogen; right: zoom in on active site Zn^{2+} ion coordinated by histidines and propeptide cysteine. SVMP propeptide-fusion expression monitored by (**e**) cell viability, (**f**) YFP fluorescence, (**g**) Western

975 blot. SVMP zymogen expression monitored by (**h**) cell viability, (**i**) YFP fluorescence (PIII
976 harvested on day 4), (**j**) Western blot analysis. SNP: supernatant+pellet, SN: supernatant, M:
977 media. Grey bars: non-toxic protein expression control, cyan: PI SVMP, green: PII SVMP,
978 magenta: PIII SVMP.
979

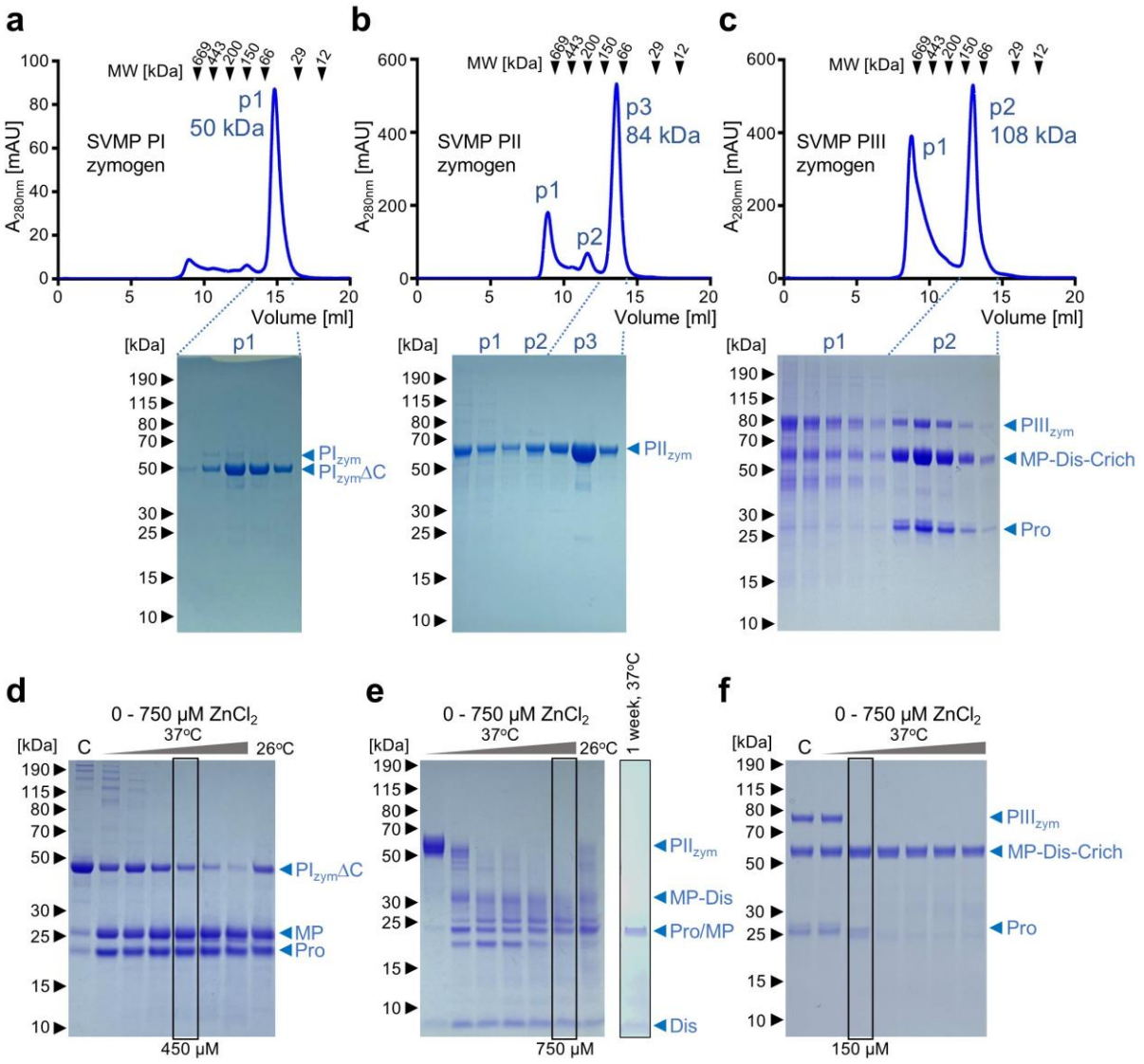

Figure 3: SEC purification of SVMP zymogens and auto-activation. Size exclusion chromatograms and SDS-PAGE of (**a**) PI zymogen ($PI_{zym}\Delta C$ lacks C terminal tags), (**b**) PII zymogen, and (**c**) PIII zymogen after IMAC and IEX. $PIII_{zym}$ partial cleavage separates the prodomain (Pro) and the mature PIII. Elution volumes of MW calibration markers are indicated in the chromatograms as black arrows. (**d**) Activation of PI zymogen into metalloproteinase and prodomain. C (control): no 18-hour incubation. (**e**) Activation of PII zymogen into metalloproteinase-disintegrin and disintegrin domain (prodomain cannot be definitively identified). After 1 week only 8 kDa and 23 kDa bands remain. (**f**) Activation of PIII zymogen into prodomain and mature PIII. At higher Zn^{2+} concentrations, the prodomain is degraded. C (control): no 18-hour incubation.

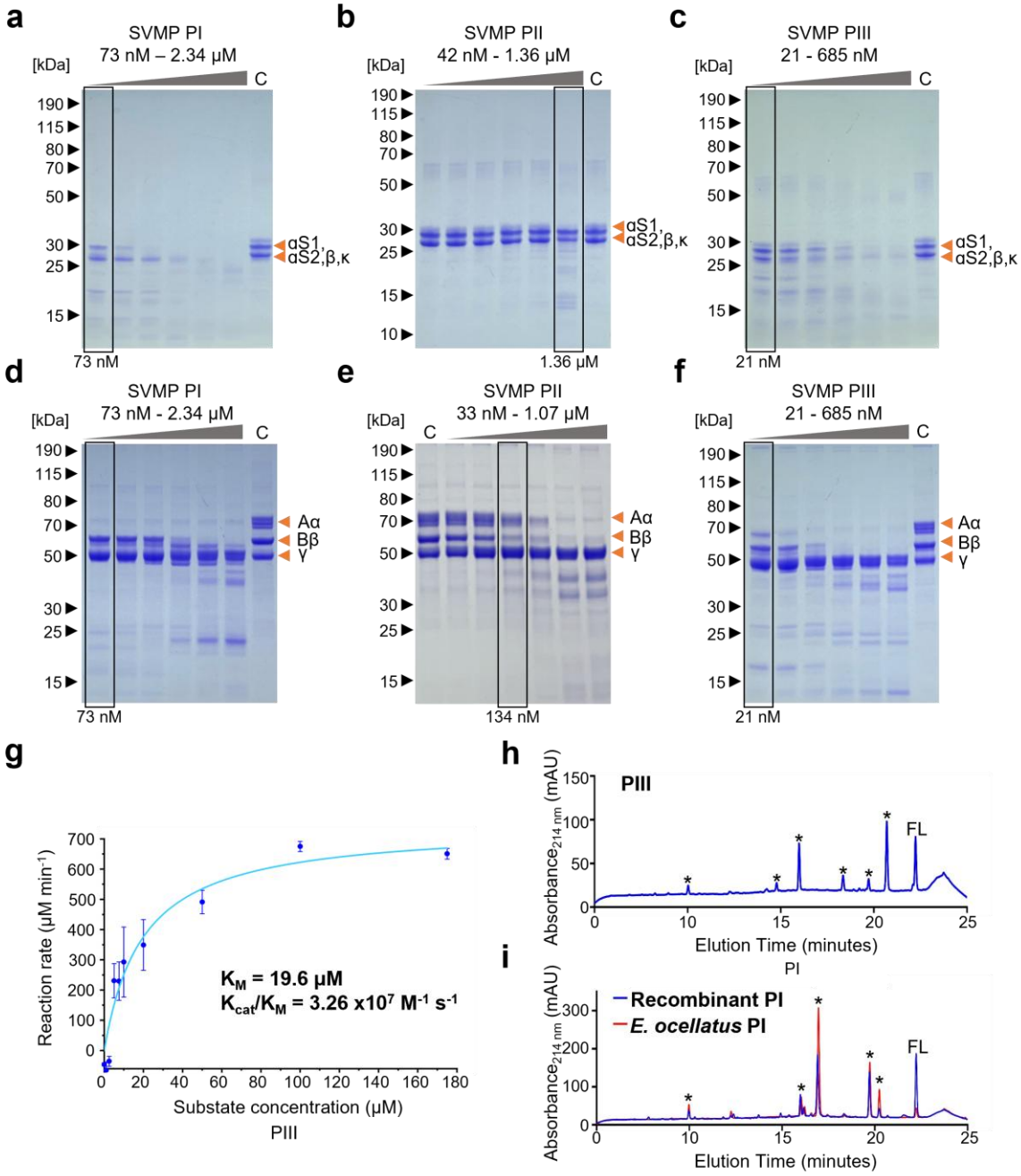

991

992 **Figure 4: *In vitro* SVMP activity and substrate specificity.** Casein degradation in the
993 presence of increasing amounts of (**a**) PI, (**b**) PII and (**c**) PIII SVMPs. Orange arrowheads:
994 domains αS1, αS2, β and κ. Fibrinogen degradation in the presence of increasing amounts of
995 (**d**) PI, (**e**) PII and (**f**) PIII. Orange arrowheads: fibrinogen chains Aα, Bβ and γ. C (control):
996 incubation in the presence of 5 mM EDTA. (**g**) PIII SVMP activity towards the fluorogenic
997 peptide substrate ES010. (**h,i**) Degradation of insulin B by (**h**) PIII and (**i**) recombinant (blue)
998 and *Echis ocellatus* PI (red). Full-length insulin (FL) and degradation products (*) are marked
999 above the peaks.

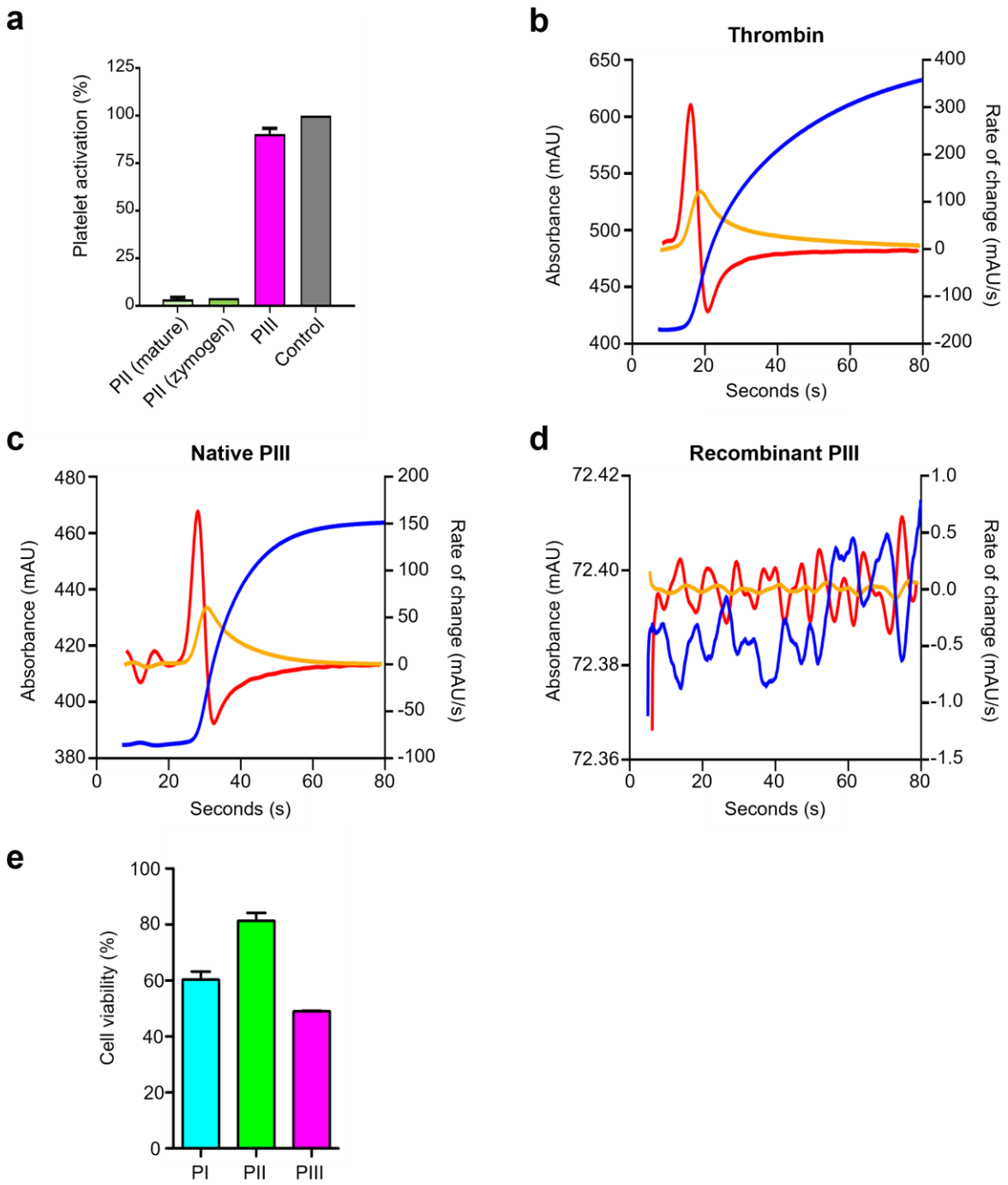

Figure 5: SVMP blood coagulation, platelet aggregation and cytotoxicity. (**a**) Inhibition of platelet activation by PII (mature and zymogen) and PIII. Control: human platelet rich plasma. Thrombin clot time assays using the ACL TOP coagulation analyser. Citrated human blood was spiked with (**b**) thrombin, (**c**) a pool of native *Echis ocellatus* PIII SVMPs, and (**d**) the recombinant PIII SVMP. Change in absorbance (blue) is plotted on the left Y axis, rate of change (1st derivative: orange; 2nd derivative: red) is plotted on the right Y axis. (**e**) MTT cytotoxicity assay showing viability compared to the buffer-only control of HaCaT cells after 24-hour incubation with activated PI, PII and PIII SVMPs.